Radiative Transfer and Thermal Performance Levels in Foam Insulation Boardstocks

by

John David Moreno

B.S.C.E. Stanford University

(1990)

Submitted to the Department of Architecture
in partial fulfillment of the requirements for the degree of

Master of Science in Building Technology
at the
Massaachussetts Institute of Technology
September 1991

Signature of Author.....
Department of Architecture
August 16, 1991

Certified by.....
Leon R. Glicksman
Professor, Building Technology and Thermal Sciences
Thesis Superivisor

Accepted by.....
Leon R. Glicksman
Chairman, Departmental Committee on Graduate Students

Radiative Transfer and Thermal Performance Levels in Foam Insulation Boardstocks

by

John David Moreno

Submitted to the Department of Architecture on
August 16, 1991 in partial fulfillment of the requirements
for the degree of Master of Science in Building Technology

Abstract

The validity of predictive models for the thermal conductivity of foam insulation is established based on the fundamental geometry of the closed-cell foam.

The extinction coefficient is experimentally and theoretically determined; the theoretical prediction based on measured geometrical properties differed from the measured values by an average of 6% for ten different foams

An approximate method uses measured geometrical values to adjust the measured diffusion coefficients of reference foams. The adjusted coefficients are used as inputs to a computer program which computes the effective thermal conductivity of the foam as a function of time. Values of effective thermal conductivity measured on laboratory and field samples are used as a standard for comparing the results of the physical models and the ageing program. Measured and predicted values differ by 11%, 13%, 1%, 5%, and 1% for the initial thermal conductivity of five foams tested. These errors decrease with time.

The ageing program is used to simulate the time-averaged performance as a function of foam density, mean cell diameter, and fractional distribution of solid polymer. The results of the simulation indicate that for a 15 year service life, the optimal density is approximately 3 lb / ft^3.

Thesis Supervisor: Leon R. Glicksman
Title: Professor of Building Technology

Acknowledgements

To the Lord: I never give You proper thanks. May you continue to bless me and my loved ones.

Thank you Mom, Dad, Albert, Sylvia, and Lionel. I love you all more than I ever care to say....

To Professor Glicksman and the Building Tech. group....thank you for your support and friendship throughout this campaign

Thank you heat transfer people. You made me really feel at home...

To the many friends I made, more power to you....

A formal thank you to the Environmental Protection Agency who funded this work (contract number CR-815210-01-0).

Table of Contents

Nomenclature

A	area
BTU	British thermal unit
C	species concentration
CFC	chloroflourocarbon
D	diffusion coefficient
E/R	activation energy
ft	foot
F	degree fahrenheit
Fo	Fourier number
f_S	fraction solid in the struts
H	hour
HCFC	hydrochloroflourocarbon
in	inch
I, i	radiant intensity
J	mass flux
k	thermal conductivity
K	extinction coefficient
L	length, thickness
LT	lifetime, service life
P	partial pressure
Pe	permeability coefficient
PIR	polyisocyanurate
PUR	polyurethane
q	energy flux
R	resistance time
RHS	right hand side
S	solubility coefficient
SEM	scanning electron microscope
S_V	surface to volume ratio
T	temperature

TI	total integration
α	absorptance
β	anisotropic correction coefficient
δ	void fraction
Φ	phase function
κ	optical thickness
σ	Stephan-Boltzmann constant
τ	transmission
ω	solid angle

Subscripts

avg	average
b	blackbody
cw	cell wall
eff	effective
f	foam
g	gas
i	element specific
I,o	initial
<l>	mean chord length
m	mean
M	measured quantity
r	radiative
R	Rosseland mean
s	scattering
s,sol	solid
T	effective time-averaged quantity
w	wall
x-s	cross sectional
λ	wavelength (spectral quantity)
$\Delta\lambda$	over wavelength region

Superscript

'	directional quantity

List of Figures

List of Tables

1.Introduction

1.1 Background

1.1.1 What is Foam Insulation?

Foam insulation is a cellular polymer material with a very large fraction of void space. Foam insulations come in various forms depending upon the application and production process. Typical uses of foam insulation are in the refrigeration and the building industry. In the appliance industry, foam insulations are formed in the cavity between interior and exterior walls of refrigerators. In-situ installation of foam insulation is done in the building industry as well. A growing application for foam insulation is in pre-fabricated building panels. The foam insulation for this application is produced in the form of panels which may be combined with other building materials to produce an effective structural and thermal building element. Foam insulation panels produced for this application are called laminated boardstocks, or simply boardstocks.

Foam insulation in the ideal sense is a highly regular network of polygonal shaped cells with polymer exteriors and gaseous exteriors [see Figure 1.1A]. The volume ratio of solid to gas is approximately 1:32. The individual cells defining the microstructure of the foam insulation are closed-cells whose edges and walls are termed struts and walls, respectively. Struts define the juncture between neighboring cells and represent localities of high solid polymer density [see Figure 1.1B]. The void space within the closed-cell is initially filled with a gas that has vaporized during the forming process of the foam. The gas composition will change with time due to gas permeating through the foam material.

The basic chemical constituents of the closed-cell foam is a polyol, an isocyanate, and a blowing agent. Additionally, other components may be added to enhance and/or retard certain properties. The reaction of formation between the polyol and isocyanate is exothermic and produces a urethane. The released heat causes the blowing agent to vaporize and the polymer to rise and expand to form the foam. The geometric scale and relative distribution of solid in the struts and edges is determined during this reaction period. Foam insulations are thermoset polymers; that is, their

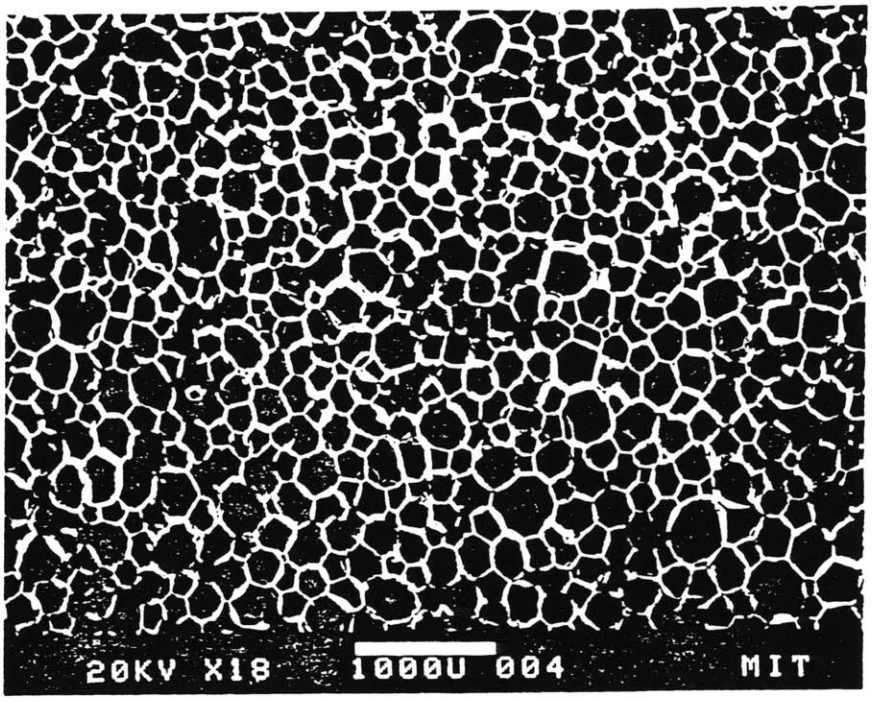

Figure 1.1: (A) SEM view of polyurethane foam insulation, (B) SEM view of triangular struts

structure is fixed once the reaction has terminated and the foam has completely expanded.

1.1.2 What is the purpose of foam insulation?

The purpose of foam insulation, and any insulation in general, is to act as a resistance to the flow of thermal energy. Many heat transfer texts employ an electrical analogy to explain the physical significance of conduction heat transfer. In this context, the material resistance to thermal energy flow is defined as inversely proportional to the material thermal conductivity. A good insulation has a high resistance to thermal energy flow; thus, insulations are materials chosen as a result of a low thermal conductivity.

Thermal performance will be defined as a level of insulating ability and will be inversely proportional to thermal conductivity. The foam insulation is initially designed for high performance. A gas blowing agent with a very low thermal conductivity is selected and will typically be a heavy refrigerant gas like CFC-11 due to its very low thermal conductivity.

1.1.3 Factors Governing Performance

Heat Transfer

Foam performance will be governed by whatever governs the foam thermal conductivity. Three separate modes of heat transfer are present in the foam insulation, these are: solid conduction along the combination wall-strut network, gaseous conduction through the closed-cell void space, and radiation. Each mode of heat transfer defines a thermal conductivity which may then be related to performance.

Mass Transfer

As mentioned, the gas composition of the closed-cell void space may change over time if gas permeation through the polymer material and foam exterior is possible. For general applications, the important gases to be considered are air and blowing agent. The polymer material is permeable by both air and blowing agent. The foam exterior is a different issue and will vary according to the intended application. In the refrigeration industry, the foam is entirely enclosed by the interior and exterior walls and tightly sealed. Gas permeation is assumed absent in the case of refrigerators since the interior and exterior walls are generally thick and very dense. However, the interior walls are permeable to air and edge joints represents locations where air may infiltrate.

In the building industry, boardstocks are typically manufactured with facer material on the exterior faces and the edges of shorter dimension are exposed foam. Facer materials will vary from manufacturer and may be composed of metal, plastic, or other materials. Ostrogorsky demonstrated the ineffectiveness of facer material as permeation barriers. His argument concerned the inadequate seal between facer material and foam polymer which would make the exposed foam edge effects more pronounced. the exposed foam edge effects. Ostrogorsky's claim is limited by the number of foams he was able to examine.

Given that the facer material is permeable to gas and blowing agent, the cell gas composition will change with time. Gas thermal conductivity is defined according to the composition of the closed-cell gas. Since the gas composition is changing with time, the gas thermal conductivity will not be constant but transient. The initial cell gas composition of 100% blowing agent will over time include air components. The trend is to increase overall thermal conductivity of the foam due to the infiltration of more thermally conductive air components. The process by which this gas exchange occurs and results in decreasing performance is called ageing.

Mass transfer is linked to heat transfer in foam insulations. Proper understanding of ageing is necessary to properly evaluate thermal performance at varying points in the foam lifetime.

1.1.4 Motivation to Improve Performance

Conservation

Insulation materials conserve energy by reducing energy load demands for a given system . The system efficiency is increased when less energy is required to sustain the same levels of output. Given that fossil fuel resources are dwindling, conservation and other measures which represent means to suppress waste and increase efficiency are very desirable.

Legislation

The Montreal Protocol is a pact signed by industrial nations aiming to reduce CFC production levels. CFC's are heavy gases which are typically used as blowing agents because of their low thermal conductivity values. It is known that CFC's are greenhouse gases and it is believed that they also contribute to ozone depletion. The Montreal Protocol calls for a 50% reduction in CFC emissions by July 1998 [1].

1.1.5 Research at MIT

The MIT foam insulation group headed by Dr. Leon Glicksman aims to broaden the foam insulation knowledge base with the goal of providing a better understanding of what governs thermal performance. Research is focused upon modelling both heat and mass transfer in foam insulations. These models are based on the fundamental closed-cell geometry and they assume one-dimensional temperature and concentration gradients (this assumption is for boardstock and typical refrigeration unit configurations). Initial heat and mass transfer models were presented by Schuetz and Reitz, respectively. Later researchers expanded upon these earlier models and devised property measurement techniques that would enhance the model's predictive power.

Currently four students, including the author, have completed foam insulation studies. Melissa Page studied the ageing of foam insulations blown with alternate gases. Arlene L. Marge has investigated the addition of small particles to the polymer mix to increase its radiative attenuation without detriment to the solid conduction. Michael Zammit is investigating the production of an insulation material comprised of powder evacuated panels (PEP) and his work constitutes an original design. The PEP's may be combined with the foam insulation to produce a higher performance insulation.

1.2 Objective

This study shall addresses two topics:

1) radiative heat transfer, and
2) predicted ageing for foam insulation boardstocks.

These two topics come together in the single goal of specifying optimal design criteria for foam insulation boardstocks based on the heat and mass transfer models.

1.3 Approach

First, the accuracy of models as predicting thermal performance will be established. The study of radiative transfer is done to establish the credibility of the heat transfer model. Further credibility of the heat transfer and ageing models are achieved by comparing theoretical prediction of effective thermal conductivity to actual measurements of effective thermal conductivity obtained from separate researchers. A

computer simulation is performed to project the ageing performance for several different panel design scenarios. The trends are used to specify designs leading to maximum performance

Five foams are studied in the effort to establish the credibility of the ageing model. Specific data relating to the mass transfer properties, in particular the permeability coefficients, of these foams was not available to the author, though data from "similar" foams was available. A method is presented that allows the permeability coefficients for the foams under study to be approximated from the permeability coefficients of the "similar" foams. This approximation relates the closed-cell geometries for the two "similar" foams and is based upon the work of Ostrogorsky. This same approximation method shall be used to generate a simulation of ageing and lifetime performance by varying the the foam properties and geometry.

2 Basic Heat and Mass Transfer

2.1 Heat Transfer

Schuetz and Glicksman developed a model based upon the three modes of heat transfer present in the foam boardstock [Eq. 2.1][2]. These three modes are conduction through the the stagnant gas, conduction along the solid polymer matrix, and radiation through the solid-gas medium. Convection within the cells is absent since it may be shown that the Grashoff number for bouyancy induced flows within the cell is too small and viscous effects dominate.[3]

The three modes of heat transfer are each represented by thermal conductivities whose sum yields a single parameter for representing total heat transfer. This single parameter is called the effective thermal conductivity, k_{eff}. For one-dimensional heat transfer through a foam insulation consisting of uniform, isotropic closed-cells, the heat transfer model states that the effective thermal conductivity is the uncoupled, linear sum of three separate thermal conductivities. The power of this model is that the heat flux through the boardstock may be determined using Fourier's law by simply taking the product of the effective thermal conductivity and the temperature gradient [Eq.2.2].

$$k_{eff} = k_g + (1 - \delta)(\frac{2}{3} - \frac{f_s}{3})k_s + \frac{16\,\sigma}{3\,K} T_m^3 \qquad (2.1)$$

where k_{eff} = effective thermal conductivity
k_g = gas thermal conductivity,
δ = volume fraction of void,
f_s = fraction solid polymer in the struts,
k_s = solid polymer thermal conductivity,
σ = Stephan - Boltzmann constant
K = total extinction coefficient of foam, and
T_m = mean temperature.

$$q = -k_{eff} \frac{dT}{dx} \qquad (2.2)$$

2.1.1 Model Assumptions

Two issues arise concerning the form of the effective thermal conductivity expression. First, are the three modes of heat transfer through the foam insulation uncoupled? Second, what significance or origin does a radiative conductivity term have?

In order to maintain a constant steady-state heat flux, it can be shown that a coupled relationship must exist between radiation and conduction [4]. The assumption of uncoupled effects is not strictly valid, though Schuetz argued that the uncoupled expression is accurate for purposes of modelling [2].

Thermal conductivity is defined by Fourier's law as the constant of proportionality between heat flux and the temperature gradient. Fourier's law is based on arguments that heat diffuses through a medium by intermolecular energy exchanges. Radiation is a form of heat transfer which does not require intermolecular actions to transfer thermal energy. Strictly speaking, radiation is not a molecular diffusion phenomenon, though an approximation may be made to the general radiative behaviour that suggests a diffusive relation and allowing a radiative conductivity to be defined. The approximation is valid in only certain limiting cases of which foam insulation is included. This approximation is called the Rosseland diffusion approximation and provides a simplification to the otherwise complex analysis of radiative transfer.

2.1.2 Time Specific Heat Transfer

The heat transfer model is only representative of one point in time. In order to achieve a representative term for the boardstock lifetime, the time dependency of the effective thermal conductivity must be determined, and integrated over the desired time span. Dividing the integrated value by the length of time (LT) gives the time-averaged value for the effective conductivity, k_{eff} [Eq. 2.3].

$$k_{eff} = \frac{1}{LT}\int_0^{LT} k_{eff}(t)\, dt \qquad (2.3)$$

Eq. 2.3 represents a time-averaged value that may easily be adjusted to account for discounting or other cost-scaling schemes which favor time-dependent value of performance.

2.2 Mass Transfer

2.2.1 Governing Equations

Mass transfer, like conduction, is a diffusion phenomena and is described as the movement of mass by molecular interactions, driven by a concentration gradient. Fick's law expresses the rate of mass transfer in perfect analogy to Fourier's law of conduction: the rate of mass flux, J, is proportional to a concentration gradient, dC/dx, and the constant of proportionality is defined as the diffusion coefficient, D [Eq.2.4].

$$J = D \frac{dC}{dx} \tag{2.4}$$

Fick's law is valid for mass transfer within a single medium. The boardstock foam represent a problem with two mediums present: solid polymer and gas blowing agent. The mass transfer for a multi-medium problem requires the use of Henry's law which defines sorption, or the ability for a species to go from one medium into another. Henry's law states that the concentration of a species in one medium (C) is the product of the partial pressure of that species (P) adjacent to the surface of that medium and the solubility coefficient (S) [Eq. 2.5].

$$C = S\,P \tag{2.5}$$

$$C \equiv \frac{n}{V} = \frac{P}{RT} \tag{2.6}$$

where C = species concentration
n/V = species number per volume
P = partial pressure
R = molar constant
T = temperature

Concentration is defined as the mass of a given species per unit volume and will have the form given by Eq. 2.6 if the gases are assumed to be ideal. Concentration is a function of temperature and pressure; species concentration increases with increasing pressure and decreasing temperature. Ostrogorsky concluded that only the pressure

gradient will affect concentration and thus drive the diffusion process; temperature differences are negligible relative to the partial pressure differences in determining concentrations. Fick's law can be rewritten to show the functional dependence on pressure:

$$J = - Pe \frac{dP}{dx} \tag{2.7}$$

where $$Pe \equiv D S \tag{2.8}$$

Fick's law written in term of pressure shows that the transport of mass is dictated by the combined effects of diffusion and sorption (i.e. permeation). This is a more acceptable form since the foam is a multi-phase system where both processes will be important in governing mass fluxes.

In mass transfer calculations, mass and pressure values are typically listed in units of cm^3_{STP} and atm, respectively. This unit convention allows the diffusion and permeability coefficients to have equal magnitude since the the solubility for all gases is 1.0 cm^3_{STP} / cm^3 atm at standard temperature and pressure [4].

Diffusion and permeation have a temperature dependence that obeys an equation of the Arhenius type:

$$Pe_{eff} = Pe_o \exp(- \frac{E}{RT}) \tag{2.9}$$

where Pe_O = initial permeability coefficient

E/R = activation energy for diffusion

This expression will be used to determine the initial permeability coefficient and the activation energy for diffusion given effective permeability values at several temperatures.

2.2.2 Successive Membrane Model

Reitz identified three mechanisms of diffusion within the foam boardstock: 1) diffusion through the gas, 2) diffusion through the cell wall, 3) and diffusion through pin-holes

or cracks in cell walls [5]. It will be assumed that pin-holes and cracks will be kept to a minimum, and it is known that the difference between diffusion through a gas is several orders of magnitude larger than diffusion through a solid. Hence, diffusion through the cell wall will govern the rate of total mass transfer.

Ostrogorsky related the diffusion coefficient to the basic cell structure. His model called the successive membrane model states that the effective diffusion coefficient is a function of the diffusion through a single cell wall and scaled by the ratio of the mean chord length to the mean cell wall thickness. This model shall be presented in full.

2.2.3 Significance of Mass Transfer

The mass transfer that is occurring is the movement of air into the foam and the movement of the blowing agent out of the foam. Neglecting the presence of facer material, gas exchange will readily occur since the solid polymer is permeable to air and blowing agent components. Partial pressure gradients drive these flows as demonstrated by Fick's law. The change of the closed-cell gas composition will consequently change the gas thermal conductivity. Since air components typically represent a threefold increase in thermal conductivity over the refrigerant gases used as blowing agents, the change to the total gas conductivity will be positive and the fraction of gas conduction heat transfer will increase.

Experience has shown that the time scale in which these gas exchanges occur is relatively short for the air components (i.e. several years) and quite lengthy for the blowing agents. We can expect to see a substantial decrease rate of decrease in thermal performance initially, followed by a gradual decrease over the remaining lifetime.

2.3 Ageing

Ageing in a closed-cell foam refers to the time dependent change of the gas thermal conductivity and represents the result of the combined effects of heat and mass transfer. Ageing constitutes an increasing gas thermal conductivity for the foam boardstock over time; this ultimately translates into a degradation of thermal performance.

2.3.1 Does Ageing Only Affect Gas Conduction ?

Given that the gas is moving through the solid polymer, at any point in time the solid polymer thermal conductivity, k_S, will be a function of that gas component within the solid polymer. It may be said that ageing of the foam may affect not only the gas conduction term, but the solid conduction term as well. The earlier assumption that gas and solid conduction are independent processes is at the base of this issue. The solid conduction term will be affected by ageing of the gas conduction term if the two are not independent of each other, but coupled. Schuetz and Sinofsky separately sought to validate the earlier assumption that the solid and gas conduction are independent of each other.

Schuetz predicted the combined solid and gas conduction and the gas conduction alone for three cases of closed-cell gas compositions. The three cases represent initial, intermediate, and terminal gas compositions over the foam boardstock lifetime. Schuetz used an expression by Russell that accounts for solid and gas conduction coupling in tandem with the Lindsay-Bromley expression which provides the gas conductivity for a mixture of gases [2]. The gas conduction value calculated from the Lindsay-Bromley expression is subtracted from the combined gas-solid conduction value using the Russell expression and the difference is the solid conduction. For cases representing different gas mixtures, the gas conduction changed as expected and the solid conduction remained essentially constant. The important finding was that the effect of coupling between solid and gas conduction is negligible and the two may be considered uncoupled.

Sinofsky utilized the transient hot-wire technique to get a direct measure of the solid polymer thermal conductivity, k_S. He performed measurements on foams of identical chemical formulation, the only difference being that one foam was fifteen years older than the other. The difference measured between the two was approximately 3% and his conclusion was that no ageing occurs in the solid polymer [6].

Schuetz and Sinofsky together demonstrated that k_S is constant over time. Changes in density are negligible and the solid polymer is not redistributing itself over time. Thus, the solid conduction term remains constant. The radiation term may be assumed unaffected by age since the sole parameter is the extinction coefficient which will be a function of the solid.

2.3.2 Ageing Program

Ostrogorsky wrote a computer code that considers the changing gas composition and computes the thermal conductivity of the gas mixture inside the foam panels. The code solves the Lindsay-Bromley expression which provides the thermal conductivity for gas mixtures [Eq. 2.10].

$$K_{mix} = \sum_{i}^{4} K_i / (1 + x_i^{-1} \sum_{j}^{4} A_{ij} x_j) \quad \text{where } i \neq j \tag{2.10}$$

K_{mix} is the resulting gas conductivity evaluated for the four gases involved in this analysis (CO_2, O_2,N_2, and blowing agent), x_i is the molar fraction of the gases, and A_{ij} is a coefficient representing dynamic viscosity, molar mass, and local temperature contributions.

Inputs into the ageing program include polymer permeability coefficients for the four gases, initial partial pressures, temperature boundary conditions, number of time iterations, and number of nodes to represent the foam panel thickness. The foam panel thickness is divided by specifying nodes since the gas mixture will not be constant throughout the foam interior. At each time step, partial pressures of the four gases are computed at each node and the Lindsay-Bromley expression is evaluated. A representative gas conductivity is the average of all the node-specific gas conductivities.

Additional inputs include the constant values of solid conduction and radiation. The time specific effective thermal conductivity is the sum of the calculated gas conductivity and the constant solid conduction and radiation values. These effective conductivity values may be inserted into Eq. 1.3 allowing calculation of the time-averaged value of effective thermal conductivity.

3 Solid Conduction

3.1 Introduction

This chapter deals with the solid conduction term as it appears in the heat transfer model shown earlier. A synopsis of the derivation shall be presented and the reader is advised to consult the original references for greater detail. The validity of the solid conduction model will be discussed.

Additionally, physical property values and geometric relations are presented that are used in the solid conduction model and elsewhere in the radiative and ageing models. These values and relations provide the inputs for the models and offer an understanding of the underlying physics involved in these models.

3.2 Solid Conduction Term

Recall the solid conduction term shown as the second term on the RHS of Eq. 2.1:

$$k_{sol} = (1 - \delta)(\frac{2}{3} - \frac{f_s}{3})k_s \tag{3.1}$$

Schuetz and Glicksman derived this expression assuming one-dimensional heat transfer through a uniform cellular matrix composed of linear and planar, solid elements. The linear elements are formed at the intersection of planar elements and are termed struts. The planar elements are the cell walls or membranes.

If the entire foam volume was solid polymer, then the solid conduction term would simply be represented by the solid polymer thermal conductivity. Since this is a far cry from reality (the solid polymer represents only a small fraction of total volume), the actual conduction term is a mere fraction of the extreme case just described.

The solid conduction term is weighted according to its relative volumetric proportion in the foam as defined by the the void fraction, δ. The void fraction is the ratio of void, or gas , volume to the entire foam volume which consists of both solid polymer and gas volumes. The void fraction subtracted from unity represents the solid

volume fraction and it is this weighting factor that is applied to the solid conduction term.

The solid conduction term is further specified by a term which represents the relative contribution of conduction through the cell walls and struts. The struts and cell walls together comprise the entire solid available within the foam and each will conduct thermal energy in a different manner.

3.3 Derivation

Schuetz analyzed this problem by first modelling the closed-cell as a cube. The six faces of the cube represent the cell walls, and the twelve edges represent the struts. Schuetz performed one-dimensional limit analyses on the cubic array of cells to determine how they conduct thermal energy according to imposed, limiting geometries: the first geometry assumed 100% cell walls and the second geometry assumed 100% struts. The results of these two extremes showed that the fractions of solid which contribute in the 100% cell wall case is 2/3 and in the 100% strut case is 1/3. Thus, twice as much heat is conducted through an all planar geometry versus an all linear geometry.

Intuitively this make sense upon observation of the cubical model shown in figure 3.1.

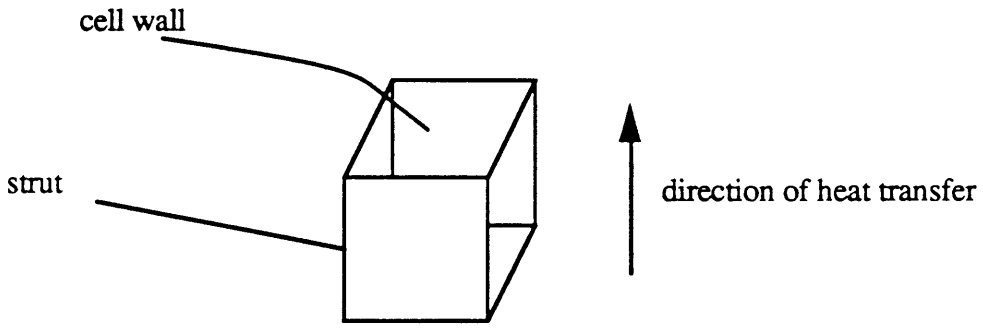

Figure 3.1: Cubic cell model

Figure 3.1 shows that four of the twelve struts are oriented in the direction of heat transfer for the given cubical cell. This analysis assumes horizontal isotherms, therefore only the struts oriented in the direction of heat transfer contribute to the total solid heat transfer: 4/12 or 1/3 of the solid is available for transferring heat in the limit of 100% struts. In the limit of 100% cell walls, four of the six walls are oriented in the direction

of heat transfer, thus 4/6 or 2/3 of the solid is available for conduction in this limiting case. These intuitive results agree with the analytical results obtained by carrying through with the one-dimensional, horizontal isotherm calculation.

Schuetz additionally presented an analysis of randomly distributed sticks and planar elements in order to provide a more realistic model of the actual foam which is certainly not cubic. The results of this analysis are identical to the results obtained in the cubic array models. Further analyses revealed that the earlier quoted numbers are in fact upper limits; a lower limit, on the order of 20% less than the upper limit, may be obtained by staggering the cubic array of cells. Schuetz suggest use of the upper limit values; this author concurs since it is better practice to under-estimate rather than over-estimate a system performance.

The fractional values, 1/3 and 2/3, represent the extreme cases which may exist in the closed-cell structure. An actual foam will have solid distributed both in the struts and in the cell walls, thus the fraction of solid contributing to solid conduction will lie somewhere between the two limiting cases. Defining the fraction solid in the struts, f_S, as giving the relative distribution of solid in the foam, then the expression $(2/3\text{-}f_S/3)$ will accurately predict the correct fraction of the solid participating in the conduction of thermal energy.

3.4 Agreement with Work of Others

Schuetz cited agreement within several percent of other researchers who performed related modelling of the solid polymer matrix [2]. Leimlich investigated the effect of cell structure in porous media as an indicator of total material properties [16]. Leimlich passed an electric current through soap bubbles and measured the electrical resistance; the measured resistance is attributed to the soap bubble matrix alone since the interior of the bubbles is non-conductive. The results in terms of the electrical conductivity are a good analogy to the thermal conductivity of the porous foam when isolating solid conduction. Leimlich's results are nearly identical to those of Schuetz.

3.5 Check of Assumptions

To reiterate, the conduction model given by k_{sol} assumes one-dimensional heat transfer and is applicable to uniform configurations of linear and planar elements. The one-dimensional heat transfer assumption is tolerable given that typical boardstocks applied as roofing panels have dimensions 4'x8'x.125'. The less tolerable assumption is that

the closed-cell configuration is uniform and geometrically isotropic. The closed-cells of the boardstock foam are elongated in shape and resemble footballs; the cells are elongated in the rise direction due to the nature of formation of the foam structure. The rise direction is typically assumed to be co-linear with the heat transfer direction for foam boardstocks, though this will vary with production process. If in fact this were true, then more of the solid polymer would be distributed in faces perpendicular to the rise direction. The higher packing density in one face results in a proportionally greater amount of solid in that face. The total heat transferred is the product of the flux and area through which the flux flows. Greater solid heat flux will be realized through foam with anisotropic geometry than foams with isotropic geometry when the direction of heat transfer and the rise direction coincide. Figure 3.2 presents a side view of an oriented geometry.

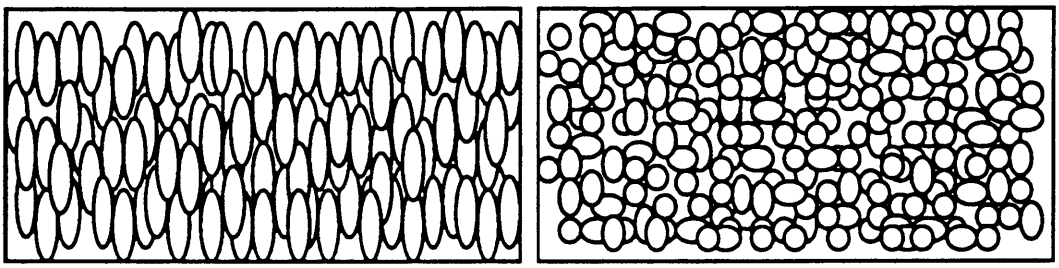

Figure 3.2: Oriented and non-oriented foam cell geometries (schematic)

3.6 Anisotropy Correction

Sinofsky presented a term which would take into consideration the effect of anisotropy which results in an increase in the heat transfer as discussed above [6]. Sinofsky proposes that an additional term be place in front of the solid conduction term as presented by Schuetz. Sinofsky suggests using the form given by Eq. 3.2:

$$k_{sol} = \beta(1 - \delta)(\frac{2}{3} - \frac{f_s}{3})k_s \qquad (3.2)$$

where β=% polymer(anisotropic) / % polymer(isotropic)

The beta term is the ratio of percentages of the polymer found in isotropic and anisotropic cases at a cross-section perpendicular to the heat transfer direction. The beta term will have a value greater than one and will increase the solid contribution.

Sinofsky's analysis hinges on the assumption that the direction of rise and heat transfer both coincide. The direction of rise will not always be perpendicular to a facer as a result of the "rolling effect" as shown in figure 3.3.

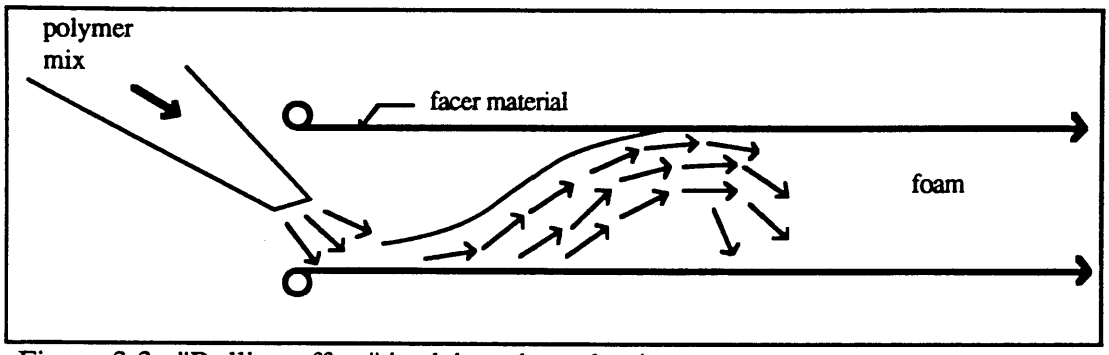

Figure 3.3: "Rolling effect" in slabstock production

The foam will rise in the direction of heat transfer until it comes up against the top boundary which in most cases will be a facer material. The reaction causing the expansion and rise of the foam is ongoing even after the foam encounters the upper boundary; as a result, the foam will continue in an oblique fashion and may "roll-over' as it encounters the boundary and take a new direction [7]. In this way, the rise of the foam is not uni-directional, but multi-directional. In light of the multi-directionality of the rise direction, the effects of anisotropy should be re-evaluated. The effects of anisotropy will be neither accounted for nor neglected until further studies are done. Glicksman is presently working on a new form of the solid conduction term to account for anisotropic cells [8].

3.7 Explanation of Variables

Four variables in the solid conduction expression variables from this expression deserve discussion, they are: the solid thermal conductivity, k_S, the void fraction, δ, and the fraction solid in the struts, f_S. Extensive work was done by Sinofsky to establish if these variables change with different forming conditions and chemistry [6].

3.7.1 Void Fraction

The void fraction is the ratio of void volume to total foam volume. An expression for the void fraction may be determined by balancing the gravity forces with the bouyant forces in air. Schuetz provides the following expression:

$$\delta = \frac{\rho_s - \rho_a - \rho_f}{\rho_s - \rho_g} \cong 1 - \frac{\rho_f}{\rho_s} \tag{3.3}$$

where ρ_s = solid polymer density
ρ_a = density of air
ρ_f = foam density
ρ_g = density of blowing agent

Typical values for ρ_s, ρ_a, ρ_f, and ρ_g are respectively 77, 0.1, 2, and 0.4 in English units of lb/ft^3. The approximate relation is valid due to the large scale difference between the solid polymer and the other densities. As mentioned earlier, typical values of void fraction are 0.97 and 0.98.

3.7.2 Fraction Solid in the Struts

The fraction solid in the struts and the fraction solid in the cell walls sum to unity. Reitz presents the mass balance for determining the fraction solid in the cell walls, f_{cw}, which may easily be extended to provide the fraction solid in the struts, f_s [5]:

$$f_{cw} = \frac{S_v\, t_{cw}}{(1-\delta)} \tag{3.4}$$

$$f_s = 1 - \frac{S_v\, t_{cw}}{(1-\delta)} \tag{3.5}$$

where S_V = surface area to volume ratio,
t_{cw} = cell wall thickness, and
$(1-\delta)$ = solid fraction.

The surface to volume ratio, S_V, is discussed in terms of a characteristic closed-cell. Exactly as its name implies, the surface area of the closed-cell area, counting one side of each cell wall, is divided by the closed-cell volume. The surface of the closed-cell multiplied by the cell wall thickness represents the volume of solid in the walls of a single closed-cell. Dividing by the total fraction of solid in the entire closed-cell (which includes struts) should describe the fraction of solid in the walls. The fraction solid in the struts plus the fraction solid in the walls must be unity.

The cell wall thickness is measured and the solid fraction is obtained by subtracting Eq.3.3 from unity.

A transient hot-wire technique was used by Sinofsky to measure the solid polymer thermal conductivity for a range of foams [6]. Twenty four different boardstock foams representing various formulations were tested. The solid polymer thermal conductivity was found to be relatively constant over this range of polyurethane (PUR) and polyisocyanurate (PIR) foams. This result supports a notion that variations in formulation translate into subtle differences for measured foam properties.

A value of 1.87 BTU in /h/F/ft^2 represents an average value of five PIR foams tested by Sinofsky. The average value for the PUR foams differs by 5%.

4 Radiation

4.1 Introduction

4.1.1 Background

Radiation energy is spectral in nature and emitted energy will span the electromagnetic spectrum of wavelengths. Thermal radiant energy is just one range of wavelengths in the electromagnetic spectrum which spans the far and near infrared, the visible, and a portion of the ultraviolet regions of the electromagnetic spectrum (i.e. from 0.01 to 1000 μm wavelengths). The temperature at which a body emits radiation will dictate the relative spectral form of that emission; as an example, bodies like the sun emit radiation at high temperatures and most of this radiation spans the visible and near infrared regions.

The radiative exchange between bodies is the net exchange of radiation emissions and absorptions. Energy leaving a body is composed of emissions and scattered values; absorbed energy is the fraction of energy striking a body which is neither scattered nor transmitted. Just as emissions are spectrally distributed, absorbed energy is also spectrally distributed and is a function of the emitting bodies temperature and the absorbing bodies material composition. The materials physical properties in large part define the optical properties which describe how a body reacts to the range of incident radiation. For radiation from one body to strike another, the two bodies must be spatially configured so that they can at least "see" each other. The view factor enters into the calculation for radiative exchanges. Bodies in full view of each other and close together will transfer proportionally more energy than bodies whose views are obstructed or shaded and are far apart. The three considerations for radiative heat transfer between bodies are: 1) the temperatures of the bodies, 2) the optical properties of the bodies, 3) and the view factor the bodies have of each other.

4.1.2 Model of Foam For Radiative Transfer

In the foam boardstock, radiation energy exchange is modelled in the following manner. The two facers represent bodies which may have the tendency to exchange radiative thermal energy provided that a temperature difference exists. The foam composed of solid polymer and gas represents an intervening medium through which radiant exchange occurs. The foam solid elements absorb radiant energy and emit energy as a function of their local temperatures. The absorptive and scattering properties of the intervening foam medium will govern the magnitude of energy exchange.

The gas is assumed to be transparent and any radiant energy attenuation and emission is attributed to the solid polymer. In the previous chapter it was shown that the solid polymer may be modelled as linear and planar elements. In the context of radiative behaviour, the liner element, or struts, are assumed to be perfect black body absorbers, and the planar elements characterized by only a slight degree of absorption.

4.1.3 Radiative Conductivity

In Eq. 2.1, Schuetz presents the radiative transfer as one of three modes of heat transfer contributing to the total heat transfer. Eq. 4.1 presents the radiative transfer contribution as derived by Schuetz and Glicksman in the terminology of thermal conductivities.

$$k_r = \frac{16\,\sigma}{3\,K}\,T_m^3 \qquad (4.1)$$

where σ = Stefan-Boltzmann constant (1.719×10^{-9} BTU/ft2 F H)

K = total extinction coefficient, and

T_m = mean foam temperature.

The extinction coefficient is the only term which is inherent to the foam; T_m and σ are irrelevant to the design of thermal insulating materials since they are external and imposed conditions.

4.2 Radiative Transport

Radiative transport is the action of energy traveling along its emitted direction in a medium it may or may not interact with. For describing the radiation transfer in the boardstock, the critical information is how the emitted energy gets from one region of he foam to an adjacent region. Application of the general transport equation to the foam boardstock will eventually reveal how the expression for radiative conductivity, given by equation 4.1, was derived.

The general equation of radiative transport is given by Eq. 4.2 [9]; The transport equation describes how radiant energy is affected as it travels through a medium along a direction *s*.

$$\frac{dI_\lambda(s)}{ds} = -K_\lambda I_\lambda(s) + \alpha_\lambda I_{\lambda b}(s) + \frac{\sigma_{s\lambda}}{4\pi}\int_{\omega_i=4\pi} I_\lambda(\omega_i)\,\Phi(\omega,\omega_i)\,d\omega_i \tag{4.2}$$

The first term on the right hand side of Eq. 4.2 represent the attenuation of the incident energy by the extinction properties of the medium and constitutes a negative change in the incident energy.

The second term represents the amount of energy which is emitted into the s direction by mass located along that direction. Energy which is attenuated and converted to internal energy may subsequently be emitted. The second term is shown in terms of the absorption coefficient (α_λ); it is written this way to show that equal magnitudes of energy are absorbed and re-emitted in order when there is thermodynamic equilibrium. $I_{\lambda b}$ is the blackbody intensity emitted by the medium at the local temperatures at position *s*.

The last term on the RHS represents what may be called "inscaterring", which is defined as that amount of energy from other directions which is scattered into the *s* direction after interacting with neighboring elements. The phase function, Φ, scales the scattering of the neighboring elements according to the uniformity or isotropy of the resulting scattered radiation. Inscatterring causes a positive change to the local intensity. Note that in the first term, K_λ includes scattering of radiation out of the direction *s*.

4.3 Diffusion Approximation

The equation of radiation transport is an integro-differential equation. It is complex to apply this equation due to the nature of the required information (in particular Φ) and the need to find I_λ for each location within the the medium and for each angular orientation. Consequently, approximations are made for varying situations which greatly simplify the analysis. The diffusion approximation is one such simplification which is valid when the local intensity within the medium is a result of local emissions only; that is, emissions from distant elements are either absorbed or scattered and consequently diminished.

4.3.1 Applicability to Foam Insulations

The requirement for applying the diffusion approximation is that the local intensities at all points along the depth of the foam be intensities emitted from neighboring elements. This requirement is met if the temperature gradient is substantially small over the mean free path of radiation, and secondly if the temperature level of the media is equivalent to that of its surroundings so that intensities from distant elements are insignificant.

The temperature gradient is very modest across the thickness of the boardstock once these temperatures are scaled down to the level of local radiative interactions. Assuming a radiative interaction distance on the order of a cell diameter, a temperature gradient of 50 degrees fahrenheit across a boardstock of 1.5 inches (or 38,000 μm), and a characteristic diameter of 500 μm, the result is a temperature gradient of 1 degree fahrenheit per cell diameter. In terms of absolute temperatures, this is an insignificant gradient.

Intensities from far away elements will be diminished if many radiative interactions occur in the intervening distance to the element of concern. The total number of radiative interactions is synonymous with the optical thickness which is defined as the product of the extinction coefficient and the medium thickness [Eq 4.3]. This product also appears in the expression for transmissivity of intensity along a given path length [Eq4.4] [9].

$$\kappa_\lambda = K_\lambda L \tag{4.3}$$

$$\frac{I_\lambda}{I_{\lambda o}} = e^{-K_\lambda L} \tag{4.4}$$

Glicksman, Sarofim, and Flik define three regions of optical thickness [10]:

$\kappa_\lambda << 1$	transparent
$(\kappa_\lambda)^2 << 1$	optically thin
$\kappa_\lambda >> 1$	optically thick

The optical thickness for a standard boardstock with a width of 1.5 " and an extinction coefficient of 50 in^{-1} is 75. In general, foam insulations are optically thick and this implies that local intensities will not be influenced by distant elements.

The diffusion approximation is applicable to foam boardstocks since conditions within the foam may be assumed dependent on local conditions only. Radiant energy exchange is likened to conduction as the flow of heat is governed by the local temperature gradient only.

4.3.2 Diffusion Expression for Radiation

Siegel and Howell [9] provide a comprehensive derivation for the diffusion approximation. The diffusion solution shows that the local intensity depends only on the magnitude and gradient of the local blackbody intensity [Eq. 4.5]. In the calculation for the radiative heat flux, the higher order terms cancel out and the result is called the Rosseland diffusion equation [Eq 4.6].

$$I'_\lambda = I'_{\lambda b} - \frac{\cos\theta}{K_\lambda}\frac{dI'_{\lambda b}}{ds} - \text{(higher order terms)} \tag{4.5}$$

$$q_r = -\frac{4}{3K_R}\frac{de_b}{ds} = -\frac{16\sigma}{3K_R}T_m^3\frac{dT}{dx} \tag{4.6}$$

where $e_b = \sigma T^4$ and $d(\sigma T^4)/ds = 4\sigma T_m^3\, dT/ds$.

The only material parameter present in the Rosseland equation is the Rosseland mean extinction coefficient, or K_R. The Rosseland mean extinction coefficient is a total extinction coefficient obtained by integrating the spectral extinction value scaled with the spectral blackbody emissive power [Eq 4.7].

$$\frac{1}{K_R} = \frac{\int_{\Delta\lambda} \left(\frac{1}{K_\lambda}\right) \left(\frac{de_{\lambda b}}{de_b}\right) d\lambda}{\int_{\Delta\lambda} \frac{de_{\lambda b}}{de_b} d\lambda} \qquad (4.7)$$

where $$\frac{\partial e_{\lambda b}}{\partial e_b} = \frac{\pi C_1 C_2 \sigma^{1/4}}{2\lambda^6 e_b^{5/4}} \frac{\exp[(C_2/\lambda)(\sigma/e_b)^{1/4}]}{\{\exp[(C_2/\lambda)(\sigma/e_b)^{1/4} - 1]\}^2},$$

and $\Delta\lambda$ is the wavelength range containing significant radiant energy at the temperature of the medium and its boundaries.

The values for the constants used in the above expressions may be found in most radiation texts.

4.3.3 Check of Assumptions

In the derivation of the Rosseland diffusion approximation, the assumption of isotropic scattering was made. Scattering is not isotropic, or uniformly distributed, within the foam since the geometry of the cells is oriented in the rise direction. An additional complication is that at the boundary, the temperature gradient is not a nominal amount. The anisotropy of the foams and the boundary effects must be accounted for in applying the diffusion approximation.

The assumption of isotropic intensity was scrutinized by Schuetz [2]. He found that the foam boardstock scatters radiation predominantly in the forward direction, which is unfortunate since it increases the radiation heat transfer. However, Schuetz also determined that foam is highly absorbing and that scattering is secondary. In the final analysis, Schuetz stated that a 10% error in the heat flux calculation may be induced as a result of using the Rosseland mean expression in the anisotropic foam boardstock. Sinofsky analyzed the effects of neglecting of the boundary effects in terms of the temperature gradient and determined that the induced error is negligible for foams with optical thickness greater than 100, and would be 7% for foams with optical thickness of 30 [6].

In summary, the diffusion approximation may be applied to foam boardstocks as long as the spectral optical thickness is much greater than unity, and if the temperature gradient across the foam is modest; both cases have been shown valid in the application to foam boardstocks. The diffusion approximation will result in a maximum error on the order of 15%.

4.4 Extinction Coefficient

4.4.1 Qualitative Discussion of Extinction

An extinction coefficient, K, will define to what degree a medium attenuates radiation as it is transported through that medium. The extinction coefficient is defined as the sum of the absorption coefficient, α, and the scattering coefficient, σ_S. The significance of absorption and scattering may be illustrated by considering a body of mass upon which radiant energy is incident. It has already been mentioned that absorption constitutes that fraction of the incident energy which is neither scattered nor transmitted; this energy is converted into internal energy and will consequently cause a temperature increase for that body. Scattering is the fraction of the incident energy which is simply re-directed or deflected by the body. The spectral form of the radiation is unchanged in this interaction. The remaining fraction of energy will pass directly through the body of mass, neither absorbed nor scattered, and will constitute the transmission, t.

A physical explanation for the extinction coefficient is that it is equivalent to the inverse of what may be called the optical mean free path or the average distance between radiative interactions. A small optical mean free path implies a high extinction coefficient. Extinction is synonymous with attenuation, and it intuitively makes sense that the intensity of radiation in a single direction will decrease with increasing number of radiative interactions.

4.4.2 Beer's Law

The extinction coefficient may alternately be defined by Beer's law [Eq.4.8]. The significance of this expression is greatest in the experimental determination of a material's extinction coefficient. It will be shown that a simple technique for measuring a foam insulation extinction coefficient exists given that Beer's law is a valid expression for this purpose.

$$\frac{di_\lambda}{i_\lambda} = -K_\lambda \, ds \tag{4.8}$$

Beer's law states that the magnitude of intensity in a given direction s will change as a result of absorption and scattering events, which summarily define extinction events, as it moves along that direction in a medium of thickness L, defined as the distance between s_1 and s_2. Spectral transmission is defined as the ratio of intensity at s_2 to the intensity at s_1 [refer to Figure 4.1].

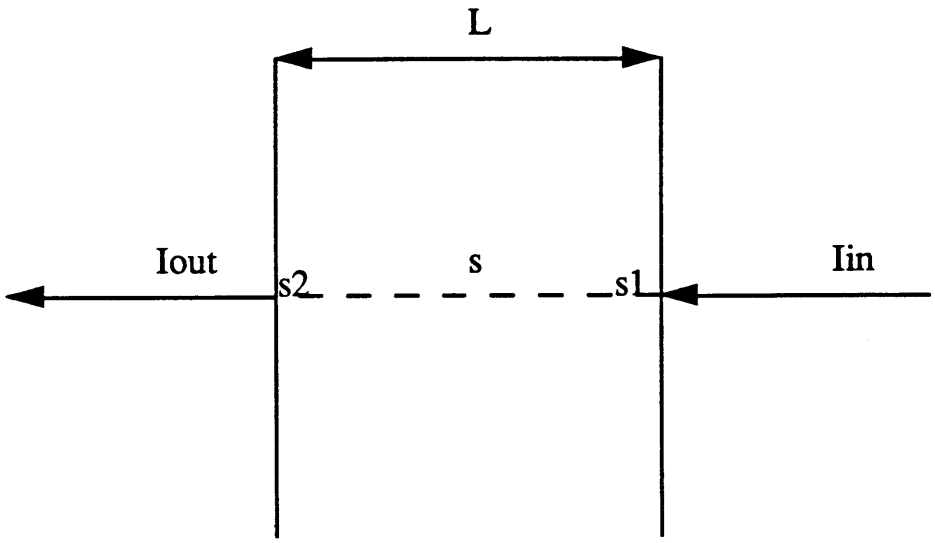

Figure 4.1: Schematic of transmission of intensity along a path *s* through a sample of thickness L.

Beer's law is simply the equation of radiative transport excluding the emission and inscaterring terms. Beer's law may be regarded as an approximate form of the general equation of transport. This approximation is valid only in the cases when the effects of emission and inscaterring are negligible relative to extinction.

A simple technique proposed by Schuetz uses Beer's law to determine spectral extinction coefficients from spectral transmission information through a given sample thickness. A spectrometer is used to determine spectral transmission and a logarithmic plot against sample thickness for a range of tested samples yields a straight line with slope equal to the spectral extinction coefficient. This technique is valid if emitted and inscatterred intensities are negligible in the spectrometer transmission determination. If either of these two terms is not negligible relative to extinction, then the measured transmission will not accurately lead to the extinction coefficient using Beer's law.

The emission term is negligible in the spectrometer for two reasons: 1) the source intensity is much greater than any intensity which may be emitted by the body at room temperature, and 2) the source of the spectrometer emits a chopped wave and the detector is properly gaged to record this transient signal; a body emission represents a a non-transient emission and would not be recorded by the detector [8].

Upon observation of the inscaterring term from the radiative transport equation, this term becomes small if the scattering coefficient, σ_S, is small or if the scattering is backward-oriented as determined by the phase function, Φ. Foams representing the greatest proportion of inscaterring are characterized by a high degree of scattering disproportionately directed in the forward direction.

The narrow-angle spectrometer is specifically designed to have a small divergence angle of detection. For inscaterring to be recorded, it must enter this narrow angle of detection; the narrower the angle, the less the measured effect of inscaterring.

Sinofsky performed a range of experiments to determine the error associated with assuming that inscaterring is negligible when using the spectrometer [6]. Sinofsky used the P-1 approximation,which considers the effects of inscaterring, to determine the extinction coefficient for foams with a range of albedos and scattering preferences. He showed that the maximum error in the calculation of the extinction coefficient attributable to the neglect of inscaterring is 11%. This translates into an overall error in heat transfer estimation of 3% if radiation is assumed to account for one-quarter of the total heat transfer in the foam insulation.

The simple technique of experimental extinction coefficient determination using Beer's law is valid since the effect of emission is negligible and a maximum 11% error due to inscaterring is tolerable.

4.4.3 Derivation of Theoretical Extinction

Theoretical expressions have been derived and are presented by Torpey and Mozgowiec,separately [11] [12]. These expressions relate total extinction coefficients for the foam boardstock with the fundamental cell geometry. It was stated that only struts and cell walls attenuate radiation since the gas is assumed transparent.

Transparent Walls

As a first approximation, the cell walls may be assumed transparent and the struts as black body (ideal) absorbers. For a black absorber, all incident energy is absorbed and

no radiation is scattered nor transmitted. The struts are modelled as linear elements as in the conduction model. The Hottel and Sarofim expression provides the extinction coefficient for attenuating linear elements, randomly oriented. The symbolic form of this expression is shown by Eq. 4.9.

$$K = C L_V Q \tag{4.9}$$

C is the projected cross section of the strut per unit length, L_V is total length of struts per unit volume, and Q is the efficiency factor. In Torpey's analysis, the struts are assumed to be triangular in shape and the efficiency factor, Q, is one since the struts are assumed black. From the foam geometry, Torpey determined values for C and L_V in terms of foam physical properties. The resulting expression for the foam extinction coefficient is given by Eq. 4.10.

$$K = \frac{4.0}{d} \sqrt{f_s \frac{\rho_f}{\rho_s}} \tag{4.10}$$

Recall that the assumptions in this derivation were: 1) the cell walls are transparent, 2) the struts are ideal absorbers, 3) the struts are randomly distributed, and 4) the struts are triangular in shape.

Absorbing, Optically Thin Walls

Schuetz proved that cell walls are not transparent by experimentally measuring the transmission of a thin film taken from a free rise bun surface of a PUR foam.

Mozgowiec performed an analysis for optically thin cell walls and assumed an uncoupled relationship between strut and cell wall attenuation. Eq. 4.11 shows the resulting expression proposed by Mozgowiec.

$$K = \frac{4.0}{d} \sqrt{f_s \frac{\rho_f}{\rho_s}} + \frac{\rho_f}{\rho_s}(1 - f_s) K_w \tag{4.11}$$

Strut extinction is the same as that presented by Torpey, and the wall contribution introduces only one unfamiliar term, K_W, which is the extinction coefficient of a single cell wall. The two terms preceding the cell wall extinction coefficient represent the volume fraction of solid in the cell walls.

Mozgowiec used the data from Schuetz's cell wall transmission measurements and determined that the extinction of a single cell wall is 1633 cm^{-1} or 4148 in^{-1}; this value is assumed to be constant for foam insulations in general. No further work has been done to verify this assumed value for the single cell wall extinction coefficient and the author considers this value suspect in the analyses to follow.

5 Gas Conduction and Ageing

5.1 Introduction

It was stated in an earlier section that the gas phase constitutes over 97% of the foam volume. The gas contribution accounts for roughly one-half the total heat transfer in the fresh foam, and this fraction becomes larger at 10 and 20 years into the foam lifetime. This large increase is attributed to the gas exchange occurring between closed-cells at the foam interior and the ambient atmosphere.

Legislative measures are resulting in the phase-out of CFC-11 which is typically used as a blowing agent for foam insulations. Proposed alternate gases are HCFC-123 and HCFC-141B. These blowing agents have higher thermal conductivities than CFC-11 and will result in a lower initial performance. Foams blown with the alternate gases are involved in this study.

5.1.1 Heat Transfer

The first term on the RHS of the heat transfer model (Eq. 2.1)is the gas conduction term. Strictly speaking, the void fraction should precede the gas conduction term analogous to the solid fraction preceding the solid conduction term. This weighting factor is usually taken to be unity as a result of the high void fraction.

In order to use the heat transfer model, the gas conductivity must be provided and this is known to be a function of time. The Lindsay-Bromley expression for gas mixtures is available to evaluate the thermal conductivity of the closed-cell gas, though this expression is useful only as long as the cell gas composition is defined. The cell gas composition is defined at points in time when the rate of gas permeation through the solid polymer is known. Thus, the necessary information for evaluating the ageing of foam insulations is the permeation rates of the air and blowing agent into and out of the bulk foam.

The bulk foam consists of cell walls, struts, and void space. Reitz stated that permeation through the cell walls is the only consideration for evaluating permeation through the bulk foam. Models have been devised to predict permeation through the

bulk foam based upon the fundamental closed-cell geometry. The model accuracies are checked by measured data. Permeation measurements represent an entire study alone and both steady-state and transient methods have been proposed; a good correlation between both methods, and the results of others was achieved by Brehm [13].

Measured permeability data for a foam insulation allows the gas composition within that foam to be determined. The cell gas composition will vary with time (t), location (L), and magnitude of permeation (D). The Fourier number (Fo) is a dimensionless quantity which shows the relative magnitude of these three quantities.

$$Fo = \frac{D\,t}{L^2} \tag{5.0}$$

The ageing program as discussed in chapter 2 properly incorporates these three issues.

In the absence of measured permeability information for a specific foam, permeabilities are approximated in order to carry through with calculations for gas conductivity. This chapter describes how approximations are made based upon the trends of diffusive behaviour given by the physical models. To this end, the successive membrane model is presented followed by presentation of the approximate method. The chapter closes by suggesting an application of the approximate methods and demonstrating the power of the ageing model. A method of determining the optimum design criteria for foams over their service life is discussed.

5.2 Successive Membrane Model

Ostrogorsky modelled the foam as a series of in-line cells or successive membranes separated by void spaces. The resistance of each membrane is analogous to a conduction resistance of the form l/(kA). The length scale l is replaced by the membrane thickness, t_{cw}, the thermal conductivity,k, is replaced by the cell wall permeability coefficient, Pe_{cw}, and the area is that of the cell wall surface. The membrane resistance to mass transfer is:

$$R_{cw} = \frac{t_{cw}}{Pe_{cw}\,A_{cw}} \tag{5.1}$$

Given that the model assumes in-line cells, the resistance of the entire foam is given as the sum of the in-series cell wall resistances. Defining n as the number of cell wall across the foam of thickness L, then the foam resistance can be represented by Eq. 5.2:

$$R_f = \frac{n\, t_{cw}}{Pe_{cw}\, A_{cw}} \tag{5.2}$$

Alternately, the foam resistance may be rewritten in the form of Eq. 5.1 after properly defining an effective permeability coefficient for the bulk foam [Eq.5.3].

$$R_f = \frac{L}{Pe_{eff}\, A_{x\text{-}s}} \tag{5.3}$$

$A_{x\text{-}s}$ is the plane cross-sectional area perpendicular to the gradient of concentration and permeation of gases. $A_{x\text{-}s}$ is a cross-section of A_{cw} and will always be less than or equal to the the cell wall area which may have curvature. Eq's. 5.2 and 5.3 are set equal to each other and an expression for the foam effective permeability coefficient is offered. The mean chord length, $\langle l \rangle$, is substituted for the ratio of sample thickness to total number of cell walls across that thickness, and the enhancement factor, ε, is inserted to represent the ratio of cell wall area to cross-sectional area perpendicular to permeation [Eq. 5.4].

$$Pe_{eff} = \varepsilon \frac{\langle l \rangle}{t_{cw}} Pe_{cw} \tag{5.4}$$

The actual value of the enhancement factor is independent of assumed cell geometry and may shown to have the value of 2. This is arrived at by considering the surface to volume ratio and Saltykov's relation shown earlier:

$$\varepsilon = \frac{A_{cw}}{A_{x\text{-}s}} = \frac{S_v\, V}{A_{x\text{-}s}} = S_v \langle l \rangle = 2 \quad \text{since } S_v = \frac{2}{\langle l \rangle} \text{ (Saltykov)}$$

The reduction of the quotient $V/A_{x\text{-}s}$ to the mean chord length is applicable only if the geometry is uniform.

Recalling the relation between diffusion and permeation and the convenience of evaluation at STP, a final form of Eq. 5.4 may be rewritten to incorporate the derived enhancement factor and the relation between diffusion and permeation [Eq. 5.5].

$$D_{eff} = 2 \frac{\langle l \rangle}{t_{cw}} Pe_{cw} \tag{5.5}$$

where D_{eff} is in units cm^2/s

The approximations made in developing the successive membrane model are:

1) voids represent the sole storage or capacitance elements; or in other words, the storage capacity of the solid polymer is negligible,
2) Henry's law is obeyed by polymers, and
3) diffusion and permeation are independent of pressure,

Brehm and Page show independently showed that the storage capacity of the solid polymer is not negligible as observed in a transient sorption test. Brehm states that as much as 40% of the gas may be stored within the solid [13][2]. Geankoplis demonstrates that assumptions 2 and 3 are valid[14].

5.3 Ageing Calculations

Mass transfer information is necessary to calculate ageing in closed-cell foams. In particular, the solid polymer permeabilities and activation energies must be known for the four gases involved: carbon dioxide, oxygen, nitrogen, and blowing agent. This study uses the ageing program developed by Ostrogorsky to predict ageing. The specific inputs into this program are not the permeability coefficient, but rather the initial permeability coefficients (P_o) shown in Eq. 2.9. A modified form of Eq. 2.9 is presented here to show how a best fit line yields the initial permeability coefficient and the activation energy (E/R) for permeabilities measured at various temperatures [Eq 5.6].

$$\ln(Pe_{eff}) = \ln(Pe_o) - \left(\frac{E}{R}\right)\left(\frac{1}{T}\right) \tag{5.6}$$

Initial permeability coefficients and activation energy are obtained by measuring permeability coefficients at three different temperatures and plotting these on a semi-log graph. The slope and y-intercept of the best fit line through the data are the activation energy and initial permeability coefficient, respectively.

Assumptions in the ageing model are that the temperature dependance of diffusion and permeation obey an Arhenius-type expression, and that the concurrent diffusion rates of separate gases are independent of each other.

5.3.1 Gas Ratios

Permeability tests may be performed for all four gases at three temperatures each to generate curves which allow determination of initial permeability and activation energy. Ostrogorsky noted relatively constant ratios betwen the diffusion rates of the gases. These trends were noticed in diffusion tests performed on both single cell membranes and bulk foams.

Constant diffusion ratios among the gases may be assumed in the absence of complete measured data. The diffusion information for at least one gas must be known and values for the other gases may be generated using constant ratios (how the single value is obtained is described in the next section). It is wise to use carbon dioxide as the gas for which a single value is obtained because measurements with CO_2 constitute greater accuracy. Rapid results are obtained when testing with CO_2 and time-dependent errors associated with the measuring apparatus can be minimized

5.3.2 "Similar" Foam Approximation

Given foam A and foam B, similar in physical properties, and with known geometrical properties (i.e. $\langle l \rangle$ and t_{cw}), it is claimed that the known diffusion coefficient for foam A may be used to determine the unknown diffusion coefficient for foam B. The successive membrane model provides the basis for this approximate method. The cell wall diffusion coefficient for foam A is calculated from known values of mean chord length and and cell wall thickness (from Eq. 5.5). The effective diffusion coefficient for foam B is obtained by applying its particular dimensions ($\langle l \rangle$ and t_{cw}) to the calculated cell wall diffusion coefficient of foam A.

This simple technique is a linear approximation according to the relative mean chord length-cell wall thickness ratios. The technique as described is necessarily constrained to diffusion of the same gas at the same temperature.

The assumption is that the single cell wall diffusion coefficients for similar foams are equal. The criteria used by the author for similarity is that the two foams be blown with the same blowing agent and that the foam densities be roughly equal. Similar densities will insure that foams with relatively similar geometries are considered. The accuracy of the approximation will improve with the lesser degree of geometry scaling necessary. The blowing agents need to be similar because they are absorbed by the polymer cell wall. The issue of solubility must not be forgotten; the absorbed gas will affect the sorption of all the participating gases, including itself.

5.4 Optimization

The purpose is to discover the thermal performance of a foam insulation as influenced by the foam material properties over a prescribed period of use. The hypothesis is that the design for foam parameters will differ when discussing the foam performance over its service life rather than its initial performance. Many performance tests are of the fresh foam; the results of these tests will not necessarily prescribe the design which will be most useful for foam insulation whose performance changes with time. Given that the solid conduction and radiation contributions are constant over time, the fractional importance of gas conduction increases. Consequently, overall design criteria should be proportioned to the relative importance of the three modes of heat transfer.

The foam physical characteristics as they affect the thermal performance is at issue here. The different modes of heat transfer are affected uniquely by changes in the foam structure and material properties as demonstrated by the heat transfer model. The goal of demonstrating optimal values for the foam material properties is only valid if the entire period of application is considered. It has been observed that the importance of solid conduction and radiation decrease over the first few years of the foam lifetime and that the effective thermal conductivity doubles. Gas conduction is the dominant term for total performance and design must be aimed accordingly.

Studies are performed isolating three physical parameters: the foam density, the mean cell diameter, and the fractional distribution of the material between cell edges and cell walls. It is believed that the foam density is a parameter that industry can readily control (this is demonstrated by noting the range of producible foam products and their densities). The mean cell diameter and the fractional distribution of solid may not be so easily controlled independent of the foam density. Though, by some chemical means (surfactants or additives) the mean cell diameter may be controlled independent of foam density. For example, if the rate of reaction or fluid viscosity is altered, it may be

possible to produce the same polymer distribution of solid between cell wall and struts, though on a different scale.

The fractional distribution of solid is an observed notion and the author feels that this can not be directly controlled. All three terms used in the optimization analysis are related in the expression for the fraction solid in the struts [Eq. 5.7]:

$$f_s = 1 - 2 \frac{t_{cw}}{\langle l \rangle} \frac{\rho_s}{\rho_f} \tag{5.7}$$

The mean chord length is directly proportional to the mean cell diameter and the cell wall thickness represents the proportionality between the competing variables in the optimization analysis.

6. Experimental Procedure

6.1. Introduction

Two procedural tasks constitute the span of this work. These two tasks are the evaluation of the foam boardstock radiative and ageing behaviour. Optimum design criteria for performance of the boardstock over its lifetime is determined from time-averageing the ageing behaviour. The optimization study is a subset of the study on ageing behaviour.

It has been shown that the extinction coefficient alone dictates the radiative behaviour, and that radiative, solid, and gas conductivity sum to define overall behaviour. The solid and radiative conductivities are constant over time and ageing is defined by the change of gas conductivity alone. The study of radiative behaviour reduces to determination of the extinction coefficient, and the study of ageing behaviour reduces to determination of the time-dependent gas conductivity.

Predictive models for the extinction coefficient and the transient gas conductivity have been developed at MIT. The confirmation of these predictive models usefulness is achieved by comparing predicted with measured values. This chapter outlines the methods and values employed in the prediction and experimental measure of radiative and ageing behaviour for foam insulations.

6.2. Measured Extinction Coefficient

Beer's law allows determination of the spectral extinction coefficient from known spectral transmission. Beer's law is an approximation to the radiative transport equation, though it was argued that transmission data for foam insulations collected from a narrow-angle spectrometer allow this approximation to provide results to within 11% [p.35].

Beer's law is rewritten to show it's significance in this analysis [Eq. 6.1]:

$$\ln(\tau_\lambda) = K_\lambda L \tag{6.1}$$

where τ_λ is the spectral transmission

K_λ is the spectral extinction coefficient, and

L is the sample thickness.

Three separate tasks are necessary to obtain the spectral extinction coefficients for foam insulations using Beer's law. These three tasks are: 1) prepare thin samples of uniform thickness, 2) secure a device to measure the thin sample transmissivity, and 3) obtain an instrument to measure the sample thickness.

Total and not spectral extinction coefficients are desired. Two techniques of obtaining total extinction coefficients from spectral information are presented.

6.2.1. Thin sample preparation

The best technique for cleanly cutting most rigid materials is one which utilizes a sharpened edge in a sawing action as opposed to a pull down action; the argument being that a pull-down action tends to crush more than it cuts. The isomet low-speed saw was an instrument used by Mozgowiec that uses a rotating diamond-tipped blade to cut thin samples. Earlier researchers even used standard meat slicers to obtain satisfactory samples. The isomet and meat slicer utilize a sawing action; in comparison, an ASTM standard for cell-diameter measurement which describes a pull-down technique when discussing sample preparation. A microtome is another pull-down cutting instrument mainly used in the biology field for its capability of slicing to thicknesses on the order of a micron.

Both the isomet and the microtome cutting techniques were available to the author and measures were obtained using both techniques. To determine the superior technique, results from both methods using the same sample are compared.

Isomet

A cylinder of approximately 1" diameter is cored from the boardstock using a drill press. The cored cylinder is sectioned into a cylinder of approximately 3/4" height. The resulting cylinder is fit into a plastic chuck with the aid of duct tape; the tape encircles the end which fits into the chuck until it becomes rigid and holds firm. The chuck is next fastened to the arm of the low-speed saw. A high-density, diamond-tipped blade is mounted onto the rotating wheel whose speed is set to 70%. The slicing is manually

controlled by lowering the arm and sample downward onto the rotating blade. A slow gradual lowering of the sample is found to provide the best results. In between cuttings, the arm is moved towards the blade and a range of thicknesses is visually maintained with the naked eye.

Dust or cut foam particulates are a problem in this technique. Residue from the cutting unavoidably collects on the surface of the sample. It was this issue that motivated the search and use of an alternate technique.

Microtome

A cylinder of approximately 2/3" diameter is cored from the foam boardstock using aluminum core barrels. The cylinder is next sectioned into cylinders of height approximately 3/4". These sectioned cylinders are mounted onto metal specimen holders using a liquid adhesive. The cutting apparatus consists of a fixed razor blade and a movable stage upon which the specimen is attached. The cutting apparatus is contained within a chamber with variable temperature control. Thin slices are obtained by manually cranking the stage and specimen up and down across the fixed razor blade. The stage may be moved towards or away from the blade by electronic control; the extent of this movement controls the thickness of the sample cut. Typically five to ten slices are cut.

Several settings are important. The microtome offers a setting for thickness control and it is important that this be set to zero. Using the microtome thickness control setting results in a non-uniform thickness across the sample and this is to be avoided.The setting for the chamber and stage mount temperatures are respectively set to -20 and -15 degrees celsius. Little difference was noted when the temperature varied plus or minus 10 degrees celsius from these settings for the foams used in this study. It may be of interest to note that in cutting foam which had additional particles added to the polymer mix, satisfactory slices were obtained only at the lowest temperature setting of -40 degrees celsius.

6.2.2. Thickness measurement

A Starret paper micrometer is used to measure the thickness of each sample after it has been tested. Due to the potential of damaging the sample slice during the thickness testing, the thickness measurement follows the transmission test. Inaccuracy in thickness measurement is due to the fact that the foam is compressible, especially at the

surface where it has been newly cut. More often than not, a reading less than the actual thickness is recorded.

Schuetz demonstrates an excellent technique for consistent, if not accurate, paper micrometer measurement for a foam insulation. He suggests averaging two measurements: the "touch" and "firm" measure of the thickness. The "touch" measure is when the sample is no longer able to slide freely in between the caliper heads. The "firm" measure is when the foam material begins to show strength and resist further compression from the caliper heads. Typically the difference noted between these two measures is one to two mili-inches.

6.2.3. Spectrometer Testing

A fourier transform infra-red (FTIR) spectrometer in tandem with an IBM software package (PCIR) are used for the transmission testing. The spectrometer test chamber consists of a source and collector of radiant intensity at opposite ends of a test chamber.

To perform a sample transmission test, first a measure with no sample present is obtained; this is called a background run. The sample whose transmissivity is desired is then inserted along the path between the source and collector. A new recording is taken this time with some of the radiant intensity being potentially absorbed or scattered by the sample. Again the spectral make-up is collected. The ratio of the sample run to the background run is the sample transmission. The transmissivity is plotted as a percentage against the spectral range given in units of wavenumbers (inverse wavelength). Since approximately 90% of thermal energy falls within the wavenumber band $2000cm^{-1}$ to $400cm^{-1}$, the plot range scale is accordingly adjusted.

During the entire time of testing the chamber is continuously being flushed with dry air. It is important that the conditions be constant in the test chamber for all the tests. Each time the chamber is opened to switch samples, the conditions of the room which vary continuously with time, are introduced into the chamber. Time is given for the chamber to purge and for control conditions to be re-imposed. Approximately twenty minutes is given initially for the chamber to be purged for a background test; thereafter, five minutes between sample tests is substantial.

6.2.4. Spectral Transmission to Total Extinction

The spectral extinction coefficient is calculated from the results of the transmision test using Eq. 6.6. It was shown that a total extinction coefficient is obtained using the Rosseland mean coefficient expression which is shown here for convenience:

$$\frac{1}{K_R} = \frac{\int_{\Delta\lambda} \left(\frac{1}{K_\lambda}\right) \left(\frac{de_{\lambda b}}{de_b}\right) d\lambda}{\int_{\Delta\lambda} \frac{de_{\lambda b}}{de_b} d\lambda} \tag{6.2}$$

where $$\frac{\partial e_{\lambda b}}{\partial e_b} = \frac{\pi C_1 C_2 \sigma^{1/4}}{2\lambda^6 e_b^{5/4}} \frac{\exp[(C_2/\lambda)(\sigma/e_b)^{1/4}]}{\{\exp[(C_2/\lambda)(\sigma/e_b)^{1/4} - 1]\}^2}$$

The constant values are: $C_1 = 0.18892 \times 10^8$ BTU $\mu m^4/(h\ ft^2)$

$C_2 = 25898\ \mu m\ R$

The Rosseland mean calculation is described in addition to another method of total extinction determination which assumes spectrally independent, or grey, behavior. The grey assumption is a good first approximation to the actual behaviour. This other method called the total integration method is discussed here and shall offer a comparison in the results section.

Rosseland Mean Extinction Coefficient

Mozgowiec wrote a computer program which uses Beer's law and the Rosseland mean coefficient expression to calculate a representative total extinction coefficient. Spectral transmission information is taken from the spectrometer analysis and used to calculate the spectral extinction coefficient using Eq.6.6. The spectral extinction coefficients are input into a routine which numerically approximates the integral given by Eq. 6.7. The result represents a single datum ($\ln\tau$ and L) in a plot of Eq.6.6 where the spectral notation is dropped. A representative extinction coefficient is the slope of the line best-fitting data points for several combinations of thickness and natural log transmission values. The program also computes a force-fit of this data. This corresponds to forcing

the line fit through the origin as would be the expected result since the form of Eq. 6.6 doe not account for a non-zero y-intercept. Checks were made to confirm the code as written by Mozgowiec.

The output of the computer program are:

K_b: best-fit total extinction coefficient,
σ_b: correlation coefficient of best fit data,
K_f: force-fit total extinction coefficient, and
σ_f: correlation coefficient of force-fit data

Total integration

The basis for the total integration (TI) method is the notion that average extinction is equal to the total extinction. The average transmission is obtained by using the integrate feature on the spectrometer software. The software computes the area above the curve on a spectral plot of transmission and calls this the integrated area. Defining the total system area as the sum of the integrated area and the area below the curve, the average transmission is then the ratio of integrated and system area, subtracted from unity [Eq. 6.3]. The average extinction coefficient is calculated from Eq. 6.1. This method is expressed by Eq. 6.4.

$$\tau_{\lambda,avg} = 1 - \frac{A_{integrated,\Delta\lambda}}{A_{system,\Delta\lambda}} \tag{6.3}$$

$$K \equiv K_{\lambda,avg} = - \frac{\ln (\tau_{\lambda,avg})}{L} \tag{6.4}$$

6.3. Predicted Extinction Coefficient

Recall the expression provided by Mozgowiec for combined extinction by the linear struts and planar cell walls [Eq. 4.11]. The three variables in this expression are foam density, mean cell diameter, and fraction solid in the struts. The fraction solid in the struts is a function of the foam density, mean cell diameter, and cell wall thickness. This may be seen by substituting Eq. 6.6 and Eq. 3.3 into Eq. 3.5. Thus, values for the following variables in the foams studied must be determined for prediction of the extinction coefficient:

ρ_f : foam density
d : mean cell diameter, and
t_{cw}: cell wall thickness.

The density of the solid polymer and the extinction of a single cell wall are assumed constant as discused earlier. These assumed constants are:

ρ_s : 77.5 lbs/ft^3
K_w: 4148 in^{-1}.

6.3.1. Foam density

Page noted a density distribution across the depth of the foam; variations on the order of 10% were typically found [1]. Due to potential inconsistencies in boardstock production methods, additional variations may be encountered. The measure sought in this study is a characteristic foam density. The average density of several cylinders with height representing the entire sample thickness provides this characteristic value.

The foam density is determined by coring a cylinder of approximately an inch in diameter from the boardstock. If present, facer material is removed. The isomet low speed saw with a diamond-tipped blade is used to remove the facer and adhering foam. Any cutting method which will result in a smooth planar surface is all that is necessary

The geometrical dimensions of the cleanly cored and cut foam cylinder are measured using calipers. Accuracy is necessary to the second decimal place and is recorded in feet. The cylinder volume is calculated using the familiar expression: $V=\pi d^2 h/4$. The weight is measured on a digital scale accurate to one-thousandth of a gram; this measure is converted into pounds. The foam density in English units is the foam mass in pounds divided by the foam volume in cubic feet.

6.3.2. Mean cell diameter

A mean cell diameter is used to characterize the cell geometry. Even though the actual geometry is polygonal and not spherical, proper extension to the actual geometry is possible using stereologic techniques developed by Underwood [15]. The techniques explained by Underwood in Quantitative Stereology allow three-dimensional extrapolations to be made from two-dimensional images. Photographs of the foam is taken using a scanning electron microscope (SEM). The SEM is used for the resulting

clarity of the photographs, though any instrument providing distinguishable cells and cell membranes may be used in this method.

Prepare Sample for SEM

Samples prepared for the SEM are sectioned from the boardstock by hand. A back-and-forth sawing stroke with an unused razor blade is found to produce the cleanest cuts. Two to three samples representing different relative orientations are cut from each boardstock. These samples are typically a quarter-inch square in dimension. The samples are then mounted onto aluminum SEM studs with double-sided tape; an electrical conduction path is provided by applying a thin strip of silver paint from the viewing surface to the aluminum base. The viewing surface is finally coated with a thin film of gold using a sputtering machine which allows the non-conductive foam surface to be viewed. Two photographs of each sample are taken with ten to twenty distinguishable cells along the long dimension of the 3"x5" photograph. This is typically achieved at a magnification of 50X.

Mean Chord Length: <l>

Underwood's statistically based method begins by drawing lines across the photo in any random or regular pattern. The length of each line is measured and the total number of intersections with cell membranes across the length of the line is counted. This is repeated for as many lines necessary to represent all the details of the photo. Each line's length is divided by the counted number of intersections; this quotient is termed the mean chord length and is particular to that line from which intersections were counted. The mean chord length for the entire geometry represented in the photo is the average of the many line-specific mean chord lengths.

In order to facilitate the mean chord length determination, a regular grid of one-hundred squares was imposed on a clear plastic pocket into which an SEM photograph could snugly slide. The grid fits smartly over the photograph and represents vertical and horizontal test lines and the number of intersections can be counted. The horizontal and vertical test lines are respectively drawn to be the same length. This allows a more systematic calculation: the intersection count for ten lines in each direction is recorded, averaged, and then divided by the respective line lengths to give a horizontal and vertical mean chord length. These two mean chord lengths are equivalent if the geometry is uniform. In the case that the geometry is oriented, alignment of the orientation is configured prior to image production so that the result will be grid lines running parallel and perpendicular to the orientation direction. Underwood provides the

following expression for evaluating oriented geometries along with Saltykov's relation for the surface to volume ratio:

$$S_V = 0.215\ S_V(\text{parallel}) + 0.785\ S_V(\text{perp.}) \tag{6.5}$$

$$S_v = \frac{2}{\langle l \rangle} \tag{6.6}$$

which combine to give

$$\frac{1}{\langle l \rangle} = \frac{0.215}{\langle l \rangle_{\parallel}} + \frac{0.785}{\langle l \rangle_{\perp}} \tag{6.7}$$

Parallel and perpendicular mean chord length measures are obtained from the SEM photos given that the test lines and oriented direction were initially aligned. Eq. 6.7 reduces to the isotropic geometry if the geometry is not oriented; consequently, Eq. 6.7 is used for all mean chord length calculations regardless of orientation.

Mean chord lengths are obtained from three different photographs representing the same foam. An average value of the mean chord lengths obtained for each photo is used as the representative foam mean chord length.

Multiplier

The mean cell diameter represents the dimension for an equivalent spherical volume to the actual characteristic geometry. Reitz provides an excellent study of the various possible geometries and a table of relations for characteristic geometrical dimensions. This study assumes the pentagonal dodecahedra as the characteristic geometry and the following surface to volume ratio is obtained based on Reitz's work [Eq.6.8][5]:

$$S_v = \frac{3.46}{d} \tag{6.8}$$

Eq. 6.8 may be combined with Saltykov's relation (Eq.6.6) for the surface to volume ratio which is independent of assumed geometry to provide a relation for the mean cell diameter. The coefficient preceding the mean chord length is called the multiplier. The multiplier will vary with assumed geometry. Eq. 6.9 provides the multiplier for the pentagonal dodechedra geometry assumed in this study.

$$d=1.73 \langle l \rangle \quad (6.9)$$

6.3.3. Cell Wall Thickness

The cell wall thickness is measured from the same samples sectioned for the mean cell diameter analysis. A direct measurement is obtained from an SEM photo which provides a test line and its length. Two to four photos were taken of cell walls for each foam The intent was to obtain an average value, though it was commonly the case that only one of these photos constituted an orthogonal view. Values reported for the cell wall thickness are suspect and a better method is needed to determine cell wall thicknesses.

It is very difficult to obtain clear images that show the proper thickness. The cell wall can be skewed in any direction and the two-dimensional image will show a thickness less than the actual thickness. It critical that the line of view be orthogonal to the photographed cell wall. Verification of an orthogonal view was being able to see both edges of the cell wall clearly.

Another issue is that the the cell wall thicknesses may vary with the length of the cell wall or chord selected. Intuitively it makes sense that as the length of the chord decreases, the cell wall thickness increases and vice versa. The bulk foam is composed of thick and thin cell walls; it is thought a mean value may be determined analogous to the notion of determining a mean cell diameter. A mean cell wall thickness may be obtained by measuring the thickness from a chord having the mean chord length. It was found that only walls from chords less than the mean chord length provided good images; it is presumed that only the thicker walls associated with the shorter chords survive the cutting procedure and SEM electron bombardment.

6.4. Measured Ageing

Measured ageing values are obtained for five foams used in this study from the published work of the Oak Ridge National Laboratories (ORNL). The ORNL study is a cooperative industry/government investigation to evaluate the validity of alternate blowing agents in boardstock insulations for roofing applications. Two tasks are being addressed in their study: the first task is to evaluate the effective thermal conductivity over time for foams exposed to field conditions over a temperature range 30 to 70

degrees fahrenheit, and the second task is to evaluate rates of ageing as a function of temperature. Published information from the first task is pertinent to this study.

Errors in measured effective thermal conductivity are associated with the accuracy of the instruments. ORNL uses two separate ASTM approved devices and reports very good correlation during calibration tests [17].

6.5. Predicted Ageing

Solid conduction (Eq. 3.1) and radiative conduction terms (Eq. 4.1) are constant over time. The heat transfer model given by Eq. 2.1 shows that these two values may be evaluated if known are the void fraction, the fraction solid in the struts, the solid polymer thermal conductivity, and the extinction coefficient. It was shown that the void fraction is a function of foam and solid polymer density (Eq. 3.3), and that the fraction solid in the struts is a function of the mean cell diameter, void fraction, and cell wall thickness (Eq. 5.7). The solid polymer thermal conductivity is assumed constant. The extinction coefficient has just been discussed and the predicted value is used in this analysis.

In total, the variables in the predictive models for solid and radiative conductivity are:

ρ_f: foam density,
t_{cw}: cell wall thickness, and
d: mean cell diameter

The variables are obtained in the fashion described in section 6.2. The values of the constant solid polymer density, solid polymer thermal conductivity, and cell wall extinction coefficient constants are:

ρ_s: 77.5 lb/ft^3,
k_s: 1.87 BTU in/h/ft^2/F, and
K_w: 4148 in^{-1}.

What remains is determination of the transient gas conductivity. It was stated that the MIT ageing program developed by Ostrogorsky and amended by Brehm and Glicksman is the proper tool for mapping the change in the closed-cell gas composition. The required inputs for this program are permeability information. Foams identical to

those being measured at ORNL are used in this ageing analysis. Permeability information is not available for these particular foams. The approximate method using similarity arguments in tandem with constant diffusion ratios is illustrated here in the context of correlating ageing predictions with measured ORNL values.

6.5.1 ORNL Foams

The ORNL foams consist of five foams representing different initial closed-cell gas compositions. These foams are labelled as foams 21, 23, 25, 27, and 28. Their initial gas compositions are:

21: CFC-11,
23: HCFC-123,
25: HCFC-141B,
27: 50% HCFC-123, 50% HCFC-141B, and
28: 65% HCFC-123, 35% HCFC-141B.

Permeability information was not known for these foams, but a search of foams tested by Page in her work dealing with foams blown with alternate blowing agents was available.

The measurement techniques of Page represent the cumulative work of previous researchers and credibility is given to her reported values. Measured values are available only for foams with a single blowing agent . Values for the blends, foams 27 and 28, are interpolated from the values of foams 23 and 25.

Selection of Similar Foams

Similar foams are selected on the basis of blowing agent and density. Foams are selected from work of Page with foams blown with alternate gases. The foams chosen as similar are:

This study	Page[1]
Foam 21	--------> Foam 1
Foam 23	--------> Foam 15
Foam 25	--------> Foam 18

The successive membrane model is used to relate measured diffusion coefficients from Pages foams to those in this study by assuming that cell wall

diffusion coefficients are equivalent for similar foams. The successive membrane model (Eq. 5.5) may then relate effective diffusion coefficients given that the mean chord length and cell wall thickness are known. These values for Pages foams (1,15,and 18) are given in Table 6.1; Page measured her values using the same techniques as the author.

Provided that the cell wall permeabilities are identical for similar foams, the effective diffusion coefficient are related simply by geometry. Page reports measured carbon dioxide diffusion coefficient for foams 1, 15, and 18 at three different temperatures. These values are shown in Table 6.2

The diffusion coefficients for similar foams 21, 23, and 25 may be obtained at these same temperatures using Eq. 5.5 given that the mean chord length and cell wall thicknesses are known. The diffusion coefficients for the other gases are generated assuming constant gas ratios. The air components exhibit constant ratios independent of temperature. The ratio of carbon dioxide to blowing agent increases with decreasing temperature. The gas ratios used are given in Table 6.4 and are based on data from Brehm [13]; these measured values of Brehm are shown in Table 6.3. No averaging scheme was consciously employed in selecting the gas ratios shown in Table 6.4. Effort was made to approximate the reported data and to avoid assuming accuracy with too many significant digits.

The inputs into the ageing program are determined using the Arhenius expression for diffusion (Eq. 5.6). The natural logarithm of the effective diffusion coefficient is plotted as a function of inverse temperature: for three points (at T=40,60, and 80), a best fit line is drawn. The slope of that line is the activation energy and the y-intercept is the initial diffusion coefficient. The ageing predictions are purely based on physical models of mass and heat transfer in this analysis.

Sample	chemistry: Iso., polyol	foam density †	mean chord length ¥§	cell wall thickness ¥
1 (CFC-11)	MDI, A	1.92	210	0.45
15 (HCFC-123)	MDI, S	1.67	296	0.47
18 (HCFC-141B)	MR, T	1.76	219	0.75

( ) blowing agent, † in units of lbs/ft^3, ¥ in units of microns, §calculated using Eq. 6.7
Polyol: A=aromatic amine-sucrose, S=sucrose, T=Terate 203-Multranol 9171
Table 6.1: Reported foam properties by Page [1]

Sample	1	15	18
Temperature (C)	D x 10^{-8} (cm^2/s)		
40	1326	3567	828
60	1908	5349	1880
80	3256	7937	2489

Table 6.2: Carbon dioxide diffusion coefficients for three foams used in "similarity" study. Values reported by Page [1].

Temperature (C)	D_{CO2} / D_{CO2}	D_{CO2} / D_{N2}	D_{CO2} / D_{CFC11}
40	3.9	26.6	558.3
60	4.4	28.9	370
80	2.9	29.7	267

§§MDI polyurethane foam labelled DB-831-26B

Table 6.3: Effective diffusion coefficient ratios for three air components and CFC-11 from measurements of Brehm [13].

SAMPLE	21,23,25
D_{CO2}/D_{O2}	3
D_{CO2}/D_{N2}	27
D_{CO2}/D_{BA} † (40)	250
(60)	350
(80)	490

† denotes values for the blowing agents, ( ) temperature in degrees celsius

Table 6.4: Constant diffusion ratios for three air components and blowing agents used in this study.

6.6. Optimization

Permeability information for foams with varying combinations of foam density, cell diameters, and fraction solid in the struts is determined from a single foam with given geometry and gas transfer characteristics using the technique described above. The goal of the study is to note trends from the ageing predictions for foams with varying geometrical properties. Foams are evaluated for their performance over a presumed service life of 15 years. To this end, time-averaging is done to provide a value of performance for the 15 year service life.

A time-averaged effective conductivity is the mean value determined from a linear average of thermal conductivity measurements over a specified period of time. The time-averaged thermal conductivity constitutes the representative thermal conductivity value over the presumed service life. This value is obtained from the ageing program which is adjusted to provide a linear average.

The data from foam 21 is used as the sample of known geometry and diffusive characteristics to generate the data for this simulation. Even though foam 21 diffusion information is approximated, this analysis simply needs a starting point. Foam 21 is selected because it represents a CFC-filled foam; accurate values are not critical.

What do the cases represent:

1) The aim is to represent cases that show levels of thermal performance for foam insulations over a presumed lifetime of 15 years. Present and presumed future levels of design are represented by these two cases.
2) Present studies indicate that alternate blowing agents (HCFC's) result in a greater fraction solid in the cell walls and less in the struts. Given that the levels of CFC use are to be frozen, the alternate blowing agents shall be at the forefront of future foam insulation designs. A 50/50 split of the solid distribution was chosen to represent the levels to be approached by the alternate blowing agents.
3) Mean cell diameters are typically from 0.3 to 0.5 mm, and the smallest closed-cells found by the author measure slightly greater than 0.2 mm. The two cases reflect these findings: existing designs should be represented by fs = 0.8 and d = 0.5mm.

7. Results and Discussion

7.1. Foam property measurements

Measured values of the foam geometry are the inputs into the predictive models. Table 7.1 provides measured values for the foam density, mean cell diameter, and cell wall thickness.

sample	blowing agent	foam density††	mean cell diameter¥	cell wall thickness¥	fs:fraction solid in struts
1	CFC-11	1.52	325	0.8	0.38
2	CFC-11	1.49	326	0.6	0.50
3	CFC-11	1.48	312	0.6	0.50
4	CFC-11	1.79	282	0.82	0.40
5	CFC-11	1.71	214	0.93	0.05
11	CFC-11	1.3	392	-	-
12	HCFC-123	1.35	468	-	-
13	HCFC-141B	2.02	338	-	-
21	CFC-11	1.86	324	0.5	0.71
23	HCFC-123	1.82	273	0.62	0.55
25	HCFC-141B	1.87	318	0.64	0.61
27	50/50 blend†	1.89	288	0.58	0.62
28	65/35 blend†	1.83	296	0.45	0.7

† the blends represent ratios of HCFC-123 to HCHF-141B, †† values in units of lb/ft^3,

¥ values in units of micrometers, or microns(μm)

Table 7:1: Measured property values for foams used in this study

The reported values represent averages of 2, 3, and 3 independent measures respectively for the foam density, mean cell diameter, and cell wall thickness.

7.2. Extinction Coefficients

7.2.1 Comparison of Total Extinction Methods

The total extinction coefficient is obtained from spectral transmission data using Beer's law. Two methods of using Beer's law to obtain the total extinction coefficient were presented: these are the total integration and the Rosseland mean methods. It was stated that the total integration method is approximate and that the Rosseland mean method should provide more credible results. Extinction coefficients obtained by both methods are illustrated in table 7.2.

Sample	Rosseland mean: K_R†§	Total integrate: K_{TI}†§	Difference ¥
21	74	75	1%
23	84	82	2%
25	72	67	7%
27	80	84	5%
28	70	70	0

† values in units of inverse inches (in^{-1}), ¥ percentage difference between Rosseland mean method and total integration method, §average best-fit values from two sets of data using microtome

Table 7.2: Comparison of Rosseland mean and total integration methods of determining a total extinction coefficient from spectral extinction coefficients.

The result of this comparison reveals that very little error is realized by the approximate method compared to the Rosseland mean method. No conclusions are made to suggest that the approximate method is valid in all cases. It may simply be the case that this particular foam chemistry and geometry combine to negate the observed non-grey behaviour. The Rosseland method is retained as the more accurate method, though it is worthy to note that good agreement is obtained by assuming grey behaviour and linearly averaging to obtain the total extinction extinction coefficient for foams 21 through 28.

7.2.2 Improved Slicing Technique

The Rosseland mean extinction coefficient is approximated using a computer program that numerically integrates Eq. 4.6. Extinction coefficients are obtained for force-fit and best-fit of data represented on a plot of log transmission versus sample thickness. The significance of these two values is illustrated in figure 7.1.

The expected result from Beer's law is 100% transmission at zero thickness. The force-fit line value corresponds to this ideal notion. Discrepancies between the best- fit and the force-fit data represent errors. Mozgowiec noted discrepancies between force fit and best fit lines with great frequency. He speculated that the cutting technique was partially, if not fully, blameworthy for this error. Mozgowiec used the isomet technique for thin sample preparation. The authors experience with the isomet suggests that Mozgowiec was correct in his claim that the cutting method could be blamed for measurement errors. The basis for this agreement is that dust and residue collected on the sample surface could easily be observed with the naked eye.

The check of these notions is made by comparing extinction coefficients obtained for the same sample by separate cutting techniques. The microtome cutting technique is used for this comparison. Two indicators of a superior method are: 1) valid at the limiting cases, and 2) consistency. The technique that offers the least discrepancy between force-fit and best-fit values, and the highest correlation coefficients will indicate the superior technique.

Table 7.3 presents the comparison between sets of data obtained for the same foams representing different sample preparation techniques. The method of thin-sample slicing represents the only difference for the values reported in Table 7.3.

Two features of Table 7.3 demonstrate the superiority of the microtome over the isomet as a method of thin sample preparation:

1) the percent difference between the force and best fit values (DIF) are low for the microtome, and consistently high for the isomet, and

2) the correlation coefficients (σ_f and σ_b) are consistently high for the microtome sets.

A particular note of worth is that the best-fit isomet value is in very good agreement with the microtome values. The force-fit value for the isomet is the source of the large overall discrepancy. If the isomet is to be used, best-fit and not line-fit data

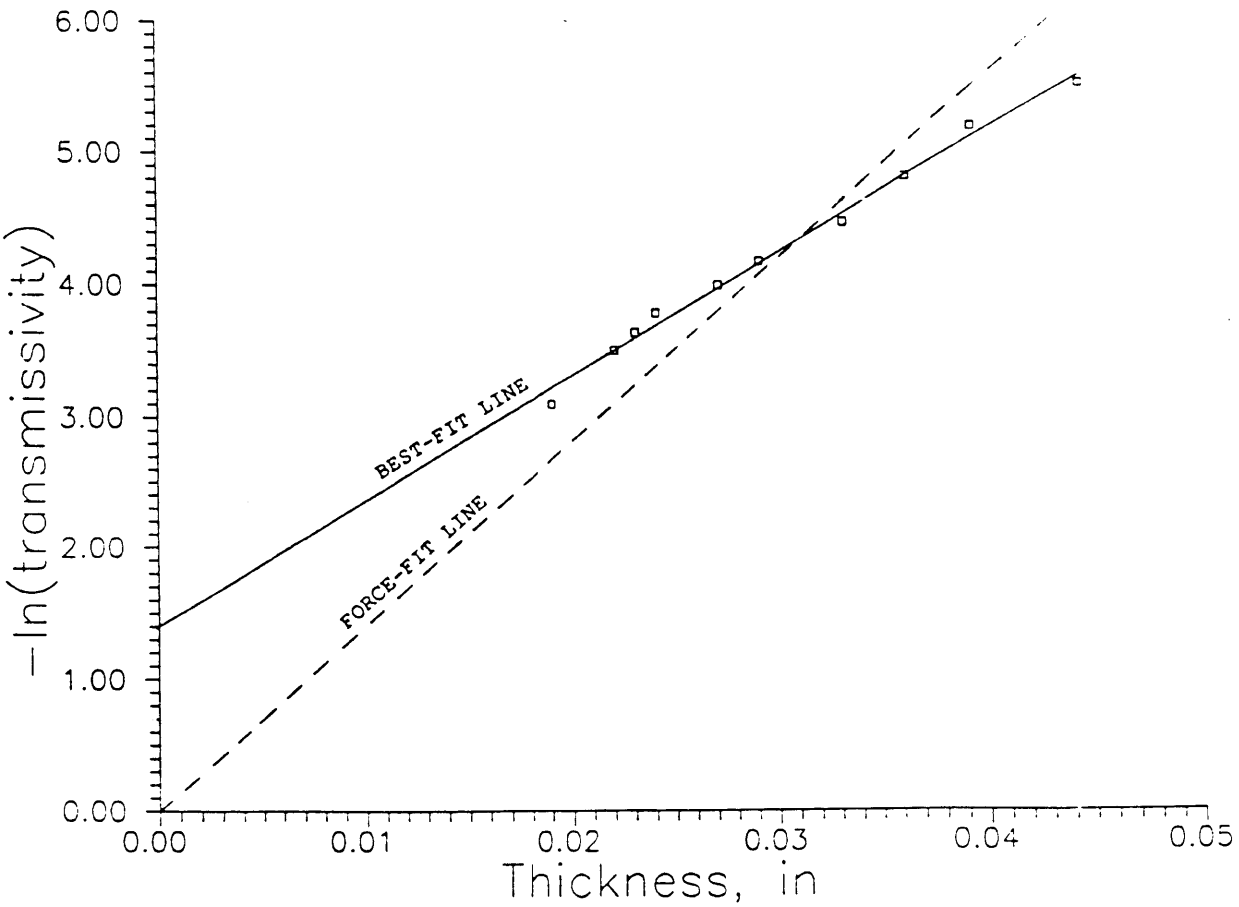

Figure 7.1: Force-fit v. best-fit slopes for calculating the extinction coefficient [12]

will provide more accurate results given that the Rosseland mean method may be used as a standard.

	ISOMET					MICROTOME				
Sample	best K_b	fit s_b	force K_f	fit s_b	DIF†	best K_b	fit s_b	force K_f	fit s_f	DIF†
21	71	0.98	98	0.87	36%	73	1.0	72	0.99	2%
23	86	0.98	97	0.97	12%	84	0.99	82	0.99	3%
25	60	0.78	92	0.58	53%	68	0.99	64	0.99	10%
27	98	0.83	100	0.83	2%	-	-	-	-	-
28	71	0.88	89	0.83	25%	67	1.0	74	0.99	9%

#all extinction coefficients in units of inverse inches, †DIF is the difference between best-fit and force-fit values for the same method

Table 7.3: Influence of thin-sample slicing technique on measured Rosseland mean extinction coefficient. (Low percentage DIF indicates more accurate measure).

7.2.3 Measured and Predicted Extinction Coefficients

The author studied thirteen foams which are used to compare predicted and measured extinction coefficients. A measured extinction coefficient is obtained using the microtome method to slice samples for testing in the spectrometer. Spectral transmission data is used to obtain the total extinction coefficient using the Rosseland mean method. The physical model presented by Mozgowiec (Eq. 4.11) is used to predict the total extinction coefficient from the following known values: foam and solid polymer density, mean cell diameter, cell wall thickness, and the extinction coefficient for a single cell wall. The cell wall extinction coefficient and the solid polymer density are assumed constant; these constant values are given in Chapter 6 (p. 51). Foam density and mean cell diameter inputs are those shown in Table 7.1.

The fraction solid in the struts has typically been assumed a constant value in past analyses [12]. From his study of CFC-11 blown foams, Reitz concluded that a reasonable assumption for the fraction solid in the struts is between 80% and 90%. Page determined the fraction solid in the struts for foams blown with alternate gases and reports values less than Reitz's recommendation [5]. Values for the fraction solid in the struts are determined upon measurement of the cell wall thickness. Measured cell wall thicknesses are reported in Table 7.1.

Table 7.4 presents measured and predicted values of extinction coefficient for the thirteen test foams. Three predicted extinction coefficients are compared with a measured extinction coefficient. The measured extinction coefficient (K_M) is the best-fit Rosseland mean extinction coefficient and will be an average value when more than one data set is available (this is the case for foams 21-28).

The first predicted extinction (K_{pI}) coefficient is based on the model given by Eq. 4.11; all values are measured including f_s. The only assumption is that the solid polymer density and single cell wall extinction coefficient have the constant values given in chapter 6.

The second predicted extinction coefficient (K_{pII}) assumes a value for the fraction solid in the struts; a value of 85% percent is used.

	measured	predicted I (fs measured)		predicted II (fs assumed=0.8)		predicted III (ORNL)	
sample	K_m	K_{pI}	% dev.	K_{pII}.	% dev.	K_{pIII}	% dev.
1	58	78	-34%	53	9%	-	-
2	66	69	-4%	51	23%	-	-
3	68	72	-6%	54	21%	-	-
4	80	91	-3%	64	20%	-	-
5	95	101	-6%	78	18%	-	-
11	55	-	-	41	25%	-	-
12	52	-	-	37	29%	-	-
13	68	-	-	61	10%	-	-
21	74	70	5%	60	19%	44	41%
23	85	86	-1%	67	21%	47	45%
25	72	78	-8%	61	16%	40	49%
27	80	82	-2%	66	18%	44	45%
28	68	73	-8%	63	7%	44	35%

**all reported values of extinction coefficient in units of inverse inches

% dev. is the percent difference between predicted and measured values

Table 7.4: Measured and predicted extinction coefficients.

The last predicted extinction coefficient is taken from the work of others studying five foams identical to those labelled 21-28. The Oak Ridge National Laboratories predict the radiative conductivity first and then solve for the extinction coefficient. The ORNL value is obtained by assuming that the radiative conductivity is the difference between the measured transient gas conductivity and an assumed value for the solid conductivity.

Figure 7.2 shows a plot of measured and predicted extinction coefficients using calculated and assumed values of the fraction solid in the struts (same notation as table 7.4). In general, better correlation between measured and predicted extinction coefficients is achieved when the fraction solid in the struts is determined and not assumed. Foams blown with CFC-11 are shown to have values of solid fraction in the struts less than values recommended by Reitz. In particular, the foams with the smallest mean cell diameter, foams 4 and 5, also have the smallest fraction solid in the struts.

An interesting observation is that foam 5 has a surprisingly low 5% fraction solid in the struts, and yet predicts the extinction coefficient to within six percent of the measured value. A quick calculation shows that the percentage extinction by the struts and cell walls is roughly 15% and 85%, respectively. The cell walls are responsible for a large fraction of the total radiative attenuation in this scenario. The validity of the calculated fraction solid in the struts is governed by the measurement of the cell wall thickness which has a large uncertainty. The measurement of 0.9 microns for the cell wall thickness raises some suspicion. It is believed that the cell wall thickness measurement was accurate, but not necessarily representative of the entire foam. Judgement can not be made at this point as to how accurate the correlations are since the cell measurement is variable.

7.3. Radiative Conductivity

Sparrow and Cunningham studied radiative conductivity and related it to the mean cell diameter [18]. The predicted effects of solid and gas conduction were subtracted from the bulk foam performance at 10 degrees celsius to provide the radiative contribution. This technique is employed for a range of reported mean cell diameters and the result is a scatter plot of nearly 80 different datum.

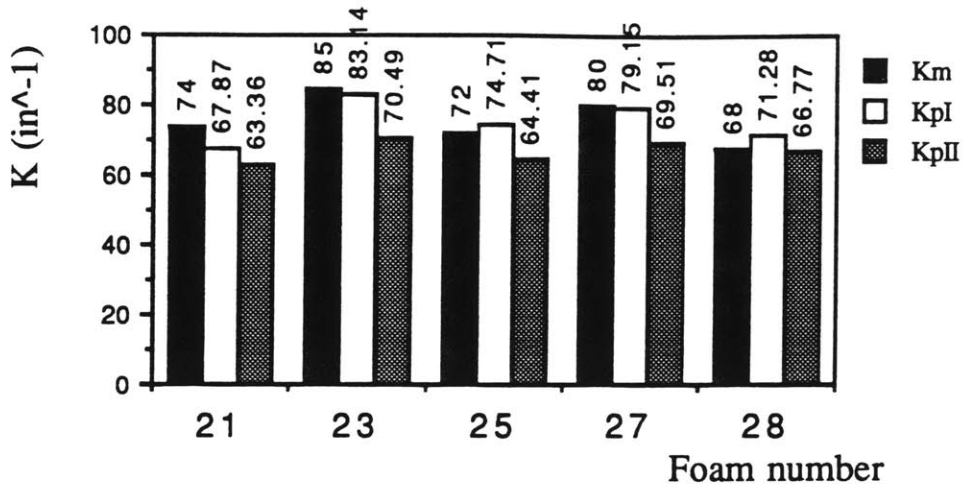

Figure 7.1: Measured and predicted extinction coefficients for foams 21 through 28

The results of Sparrow and Cunningham's study is shown by figure 7.3. Added to this plot are two theoretical curve: one curve represents radiative attenuation by struts only (from Torpey's work: Eq 4.10) and the second curve represents attenuation by struts and cell walls (from Mozgowiec's work: Eq. 4.11). In the theoretical curve, radiative conductivities (Eq. 4.1) are evaluated at 10 degrees celsius, a density of 2 lb/ft^3, and a 0.8 fraction solid in the struts is assumed.

The plot of radiative conductivity against mean cell diameter reveals that at small cell diameters, the radiative behaviour is governed by the struts and that this effect decreases with increasing cell diameter. A result from the previous section may be discussed in the context of Figure 7.2. Foam 1 is shown to have the greatest error in predicting the measured extinction coefficient. Foam 1 is characterized as having a relatively large cell diameter and a large percentage of the polymer in the cell walls. Accordingly, the predictive model for extinction coefficient shows that attenuation is dominated by the the low fraction solid in the struts probably caused small cell sizes. Hence, the predictive model for the attenuation by cell walls governs the overall extinction coefficient prediction for foam 1.

The inaccuracy obtained in the extinction coefficient prediction may be blamed on the inaccuracy of the wall model. The extinction coefficient for a single cell wall is the most suspect term in the expression for the wall model. Figure 7.4 represents a rescaling of the theoretical curve using a single cell wall extinction coefficient of 1100 cm^{-1} (2800 in^{-1}) as opposed to the value of 1633 cm^{-1} (4150 in^{-1}) used in the theoretical curve for Figure 7.3. The value of 1100 cm^{-1} is a value suggested by

Glicksman that has been shown to correlate well with earlier absorption studies performed by Sinofsky [8].

The data of Sparrow and Cunningham is of uncertain accuracy. It is believed that the predicted gas and solid conduction terms subtracted out did not incorporate ageing effects. In part this explains the large difference between their data and theory. The value for the single cell wall extinction coefficient is highly suspect. Glicksman has investigated this in light of earlier absorption studies performed by Sinofsky and suggests a value of $2800in^{-1}$ for the cell wall extinction coefficient. Figure 7.3 redraws the theoretical curve assuming this new value.

The data of Sparrow and Cunningham provides a useful trend of radiative behaviour with cell diameter and substantiates consideration of the cell wall as an attenuator of radiation. Though before any firm conclusions can be made, a concentrated effort needs to be given to discover the magnitude of single cell wall extinction coefficient.

7.4. Ageing

The successive membrane model is used to argue that unknown permeability coefficients may be obtained from similar foams whose permeability coefficients are known. The assumption is that for similar foams the cell wall permeability coefficients per unit thickness are essentially equal. The permeability coefficients obtained using this similarity argument are then used to obtain the initial permeability coefficient and the activation energy from a log permeability plot against the inverse of temperature (Eq. 2.9). The initial permeability coefficients and activation energies for the three air components and blowing agent are input into the ageing program which determines the transient thermal conductivity of the closed-cell gas at several points along the depth of the foam. A representative thermal conductivity is obtained by averaging the values at the various specified depths. The output of the ageing program is the transient thermal conductivity of the foam which may be added to constant solid conduction(Eq. 3.1) and radiative conductivities(Eq. 4.1) to give the effective thermal conductivity for the foam sample.

Similar foams were identified for foams 21, 23, and 25 whose permeability coefficients are unknown. Interpolations are made for the blends based upon their ratios with foams 23 and 25. Concurrent study of foams 21 through 28 are being conducted at the Oak Ridge National Laboratories. ORNL has published measurements of the

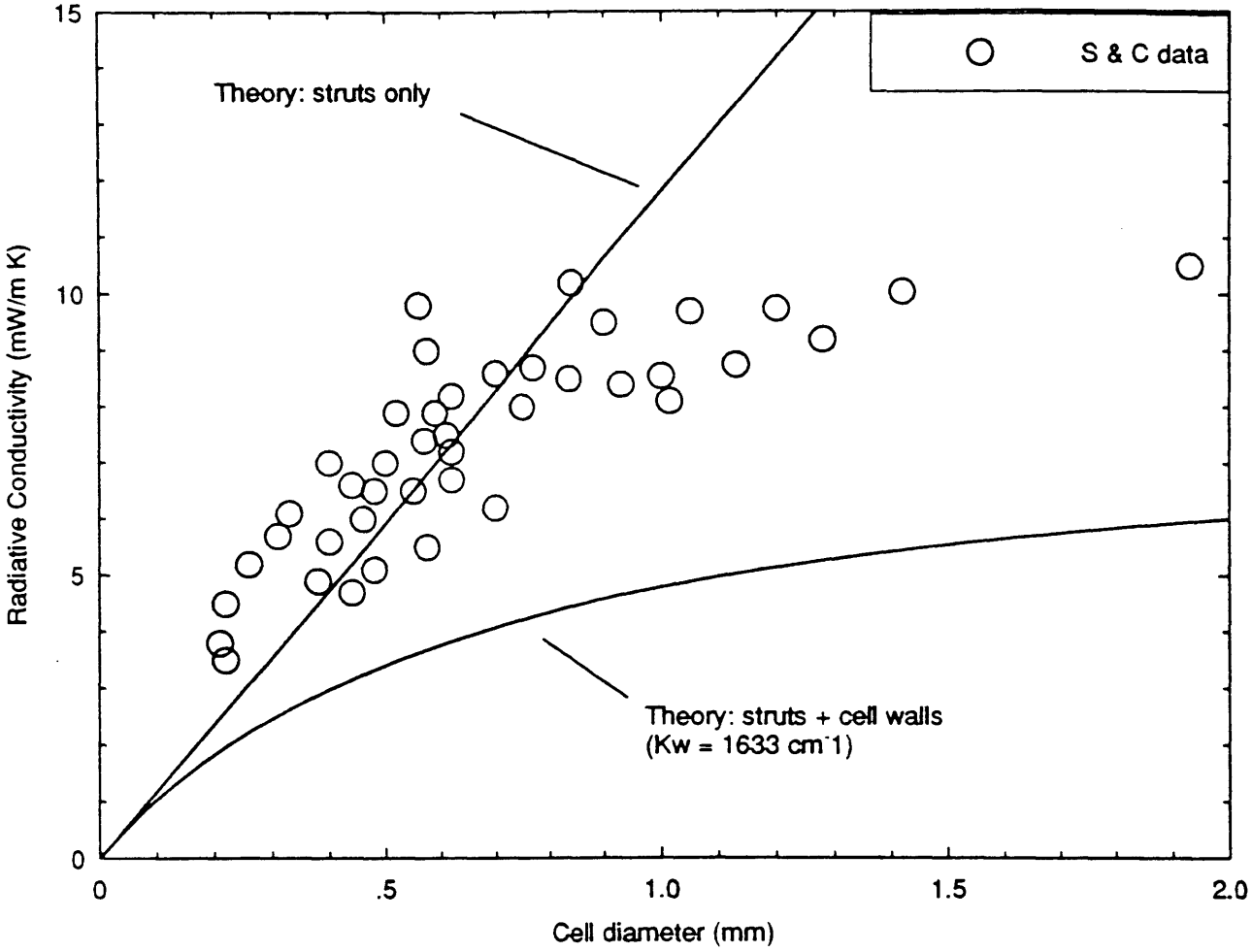

Figure 7.3. Radiative conductivity v. cell diameter. Sparrow and Cunningham data and theoretical curve (Eq. 4.1) assuming f_s=0.8, ρ_f = 2.0 lb/ft^3, T_m =10 C, and K_w=4148 in^{-1}

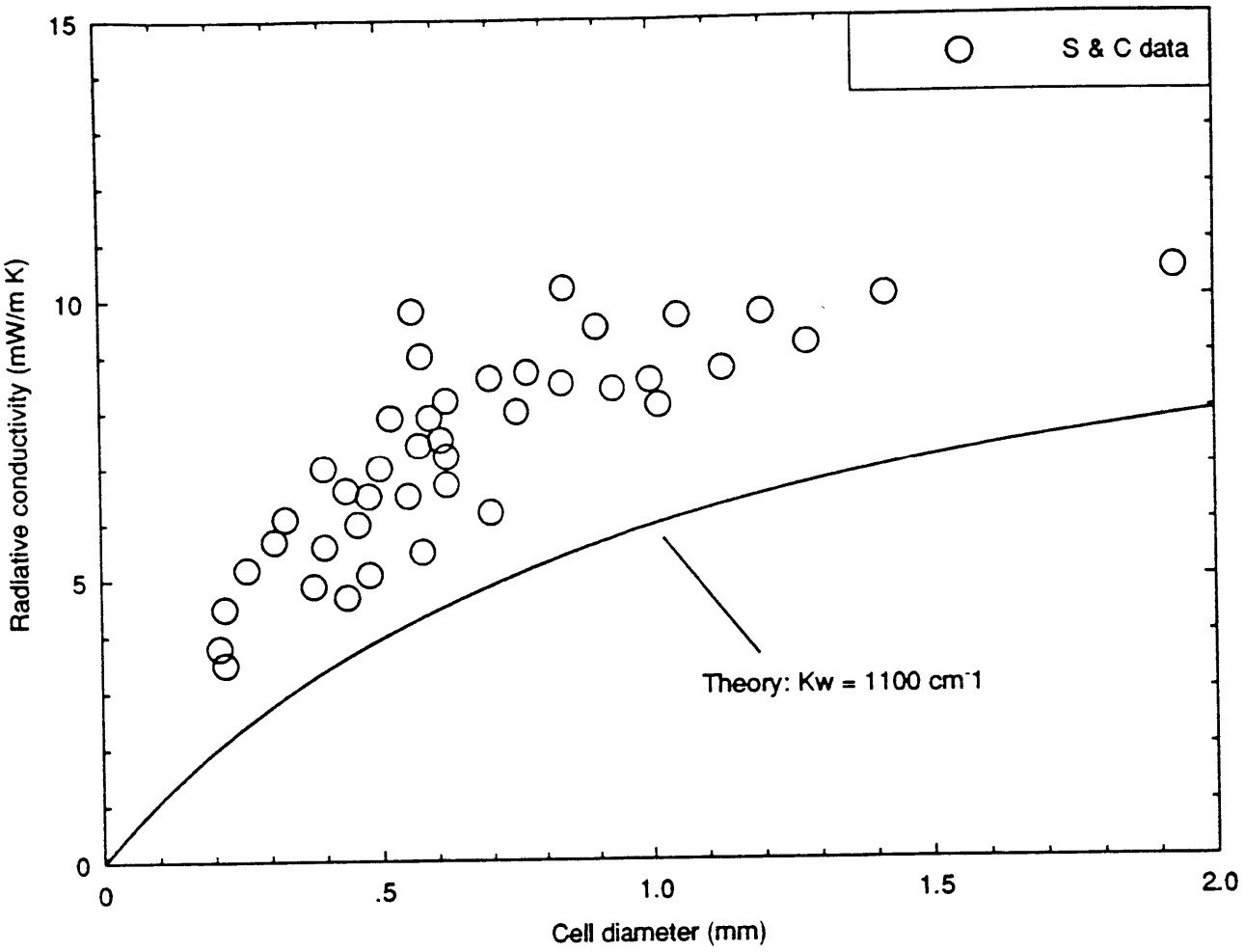

Figure 7.4. Radiative conductivity v. cell diameter. Sparrow and Cunningham data and theoretical curve (Eq. 4.1) assuming f_s=0.8, ρ_f = 2.0 lb/ft^3, T_m =10 C, and K_w=2800 in^{-1}

foam effective thermal conductivity at different times ranging from two weeks to two years [17]. Values are determined using the ageing model for at these particular points in time and a comparison is made.

Measured and predicted values are shown in Table 7.5. The predicted value represents diffusive behaviour, radiative behaviour, and solid conduction modelled as a function of the basic geometry values listed in table 7.1.

sample	age(days)	measured kT †	predicted kT †	% difference
21	65	0.128	0.143	11%
	332	0.139	0.159	15%
	532	0.156	0.165	5%
23	71	0.135	0.153	13%
	336	0.15	0.166	11%
	534	0.163	0.171	5%
25	81	0.144	0.146	1%
	340	0.156	0.161	3%
	524	0.17	0.165	3%
27	12	0.135	0.129	5%
	312	0.163	0.164	0
28	18	0.136	0.135	1%
	314	0.165	0.165	0

†KT is effective conductivity over Time and is in units of BTU in/F/H/ft2

Table 7.5: Predicted ageing v. measured ageing for foams 21 - 28.

A very good correlation is observed in Table 7.5 considering the approximations made in defining the diffusion characteristics. The values that show the worst correlation represent the samples that should provide quite the opposite effect. Known foam data from similar foams were obtained for samples 21 through 25. It is surprising that samples 27 and 28 gave closer agreement betwen theory and data than samples 21 through 25 since the former's diffusion characteristics were obtained by interpolation.

Large discrepancies were observed at the start of the foam lifetime and diminished over time. These initial errors may be attributed to the constant solid

conduction and radiation terms whose influence diminishes over time with increasing gas conduction.

It is believed that this approximate method substantiates the ability of the ageing program to predict the change of the closed-cell gas composition. Moreover, a method for approximating diffusive behaviour based on physical arguments has revealed its validity. This result shall be used in the next section to suggest optimum design ranges over a foam service life.

7.5 Optimization

The optimization is a simulation of time-averaged effective conductivities for foams with varying combinations of foam density, mean cell diameter, and fraction solid in the struts. An initial permeability coefficient is obtained from the ageing analysis; foam 21 is selected since it represents a CFC-filled foam with adequate data available (i.e. diffusion and geometry information). Permeability coefficients are generated with the assumed geometries and the initial permeability coefficients and activation energies for the gas components are obtained.

Figure 7.5 illustrates the ageing simulation performed. Graphed are the cases representing fixed solid fraction in the struts versus density range for three different cell diameter scenarios. The graphs bring to light the following:

**Reduction of the mean cell diameter is desired.With fixed f_S, at any given density the cell diameter and the cell wall thickness are indirectly proportional; the surface area of the wall increases with diameter and the thickness must decrease if a constant volume of solid in the wall is to be retained. A doubling of the cell wall thickness results in a 4 times decrease in the diffusion coefficient according as shown by the Fourier number (Eq. 5.0).

**At 50% fraction of solid in the struts, the graphs reveal that an optimum foam density exists for the CFC-filled foam at or around a foam density of 2 lb/ft^3.

**At 80% fraction solid in the struts, the optimum foam density drifts from a low of 1.75 lb/ft^3 to a high of 2.75 lb/ft^3 as the mean cell diameter increases from 0.1 to 0.5 millimeters.

The most dramatic result of this simulation is to reveal that the design criteria for the initial thermal performance is noticeably different than the design criteria for the long term thermal performance, in this case a 15 year service life (see Figure 7.5). Over the foam insulation service life, heat transfer by gas conduction represents a large fraction of total heat transfer (see figure 7.7). Thus, inhibiting gas exchange should be the top priority in designing foam insulation for service-life performance.

At a fixed solid fraction in the struts, increasing the density results in more solid in the cell wall to inhibit diffusion. Figure 7.6 shows that the long term thermal performance is optimized at a density of 2.75 lbs/ft^3 compared to the initial performance optimized density at 1.9 lbs/ft^3.

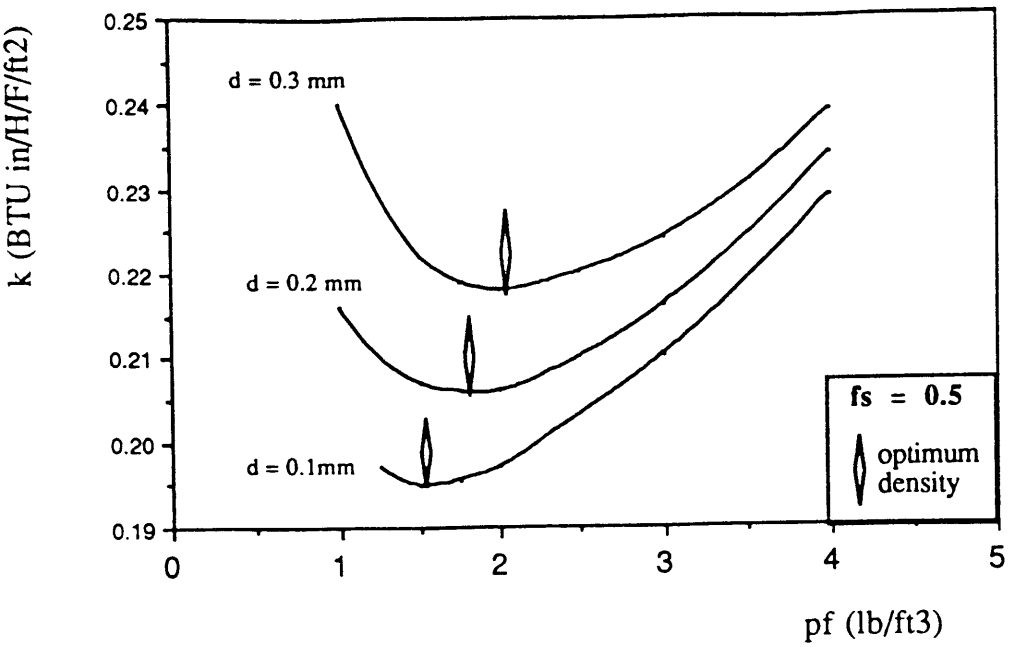

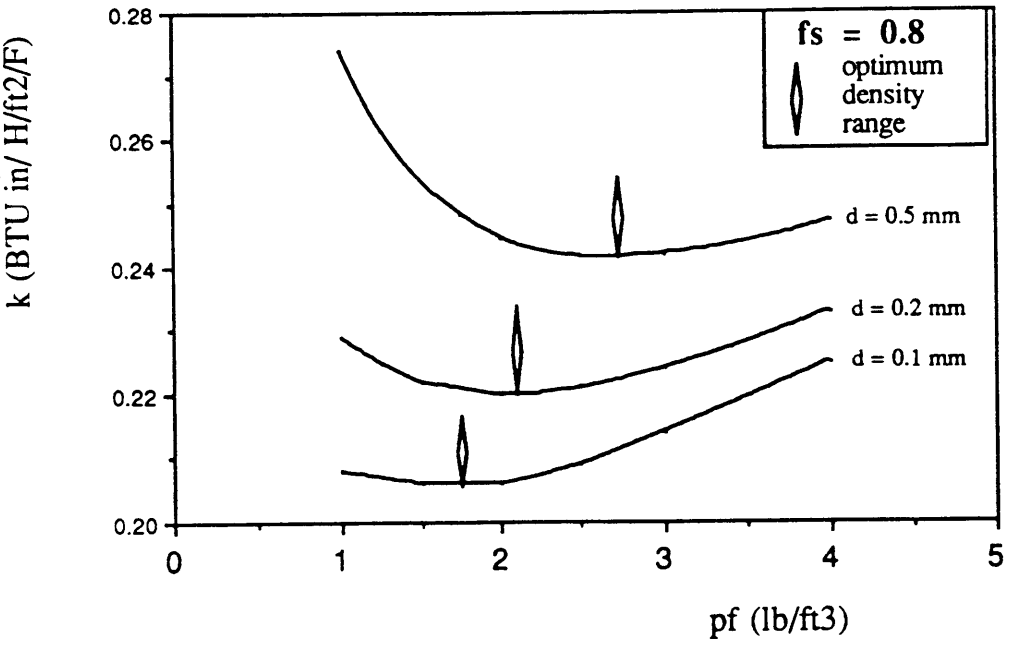

Figure 7.5: Ageing simulation for CFC filled foams: time-averaged thermal conductivity (Eq. 2.3) v. foam density.

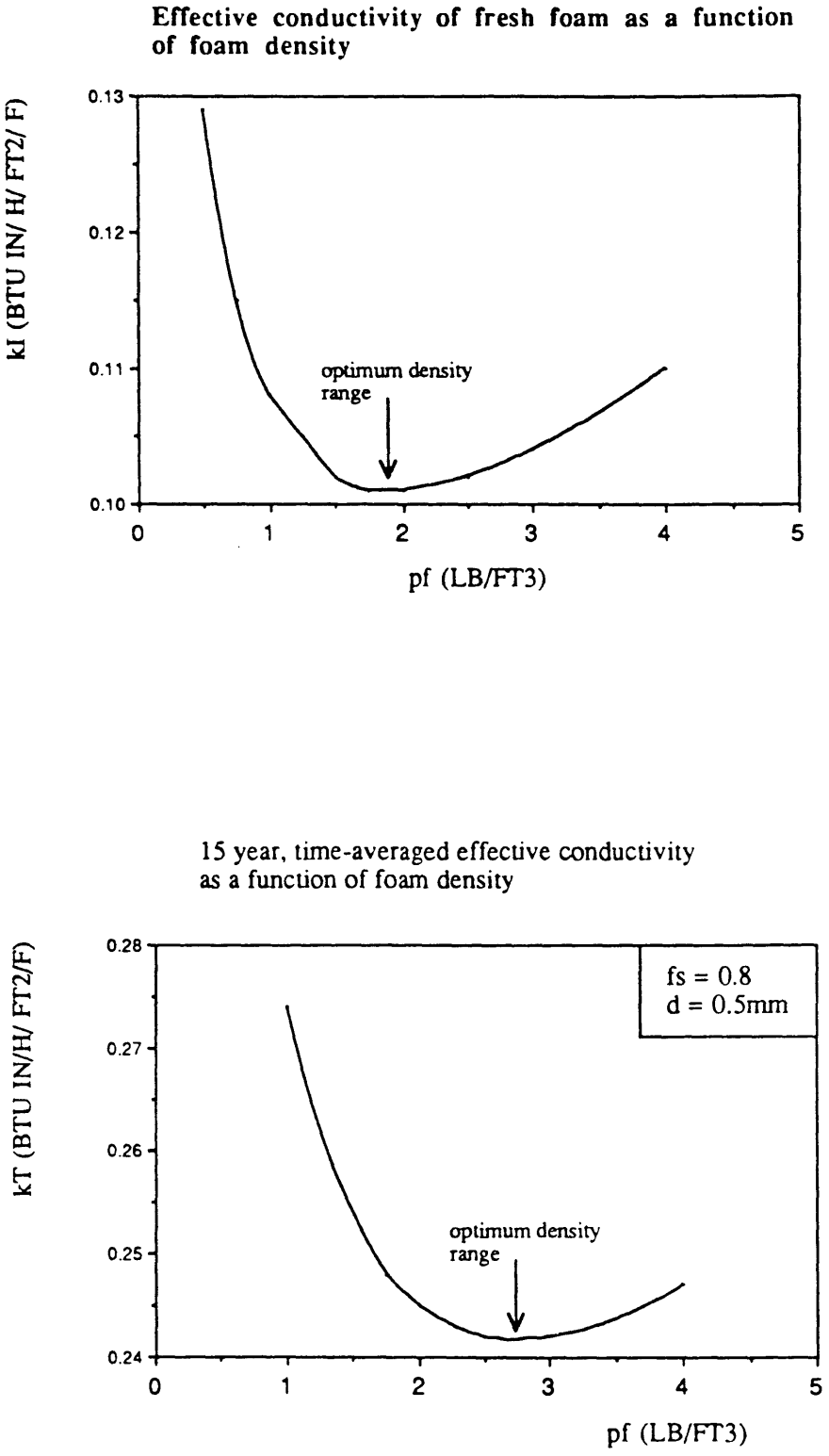

Figure 7.6: Optimum density designs for initial and 15 year, time-averaged performance.

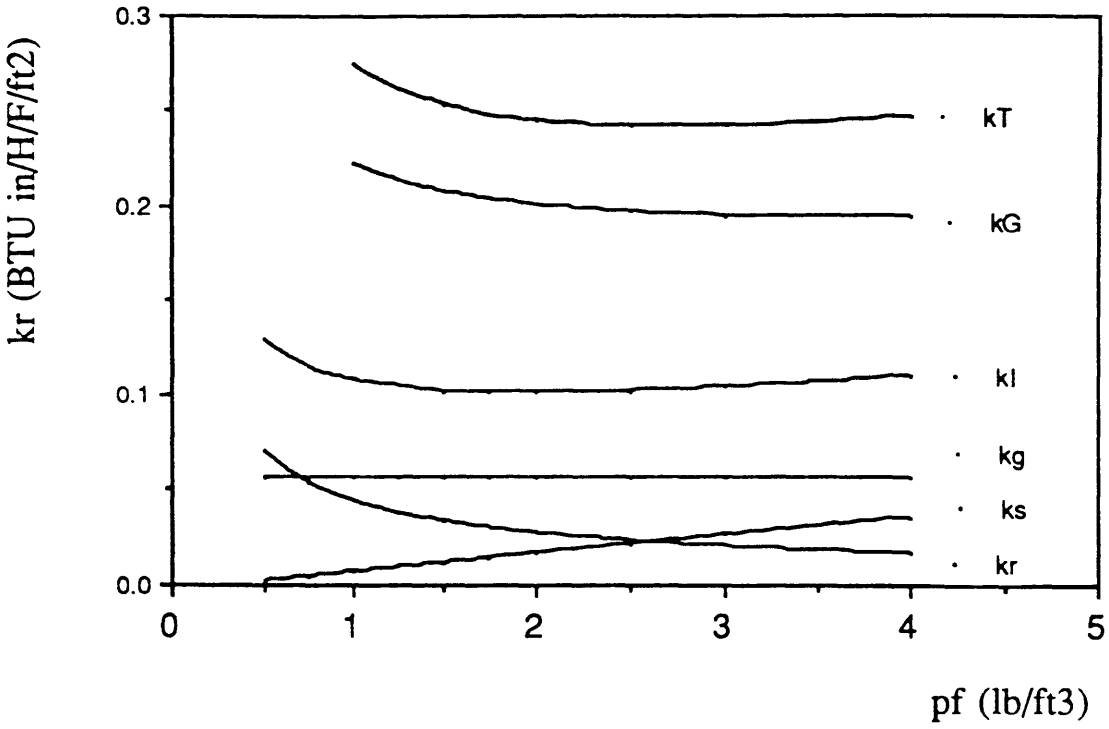

kT: time-averaged, effective conductivity (Eq. 2.3)(Eq. 2.1)
kg : time-averaged, gas conductivity (kT - kg - kr)
kI: effective conductivity of fresh foam (Eq. 2.1)
kg,i: initial gas conductivity (k_{CFC} = 0.057 BTU in/F/H/ft2)
ks: solid conductivity (Eq. 3.1)
kr: radiative conductivity (Eq. 4.1)

Figure 7.7: 15 year, time-averaged performance for a CFC-11 filled foam as function of foam density. (f_S = 0.8, d = 0.5mm)

9. Summary

The heat transfer and ageing models have demonstrated their value as valid predictors of thermal performance in foam insulations. Listed below are the salient findings of this study:

1) The microtome sample preparation method provides results that demonstrate better data fit and correlation with theoretical expectation. Though, regardless of cutting technique, a best-fit of data plotted according to Beer's law will provide consistent extinction coefficient values.

2) The fraction solid in the struts should be measured as opposed to approximated. Agreement between measured and predicted values of extinction coefficient improve dramatically when measured values of f_s are used in the theoretical expression (Eq. 4.11) instead of an assumed 80% value.

3) The foams in this study revealed small fractions solid in the struts. The cell wall thickness measure is very difficult using the present method of slicing with a razor blade and viewing with an SEM. Improved methods for measuring the cell wall thickness must be sought. Investigation may entail studying the related behaviour between wall thicknesses and chord lengths. If trends can be noted between these two, then scaling may be possible from thicknesses measured at short chord lengths to the desired mean chord length.

4) The work of Sparrow and Cunningham verify the importance of the cell walls in attenuating thermal radiation. The term of greatest importance in predicting the magnitude of wall attenuation is the single cell wall extinction coefficient; the value of this term is uncertain.

The foaming process must be investigated; studies may involve simulating the foaming process on a larger scale to produce walls with identical thermal history as those on the smaller scale to be measured in the spectrometer.

5) Ageing studies are inconclusive due to uncertainty associated with measured f_S. Very good agreement obtained using approximate methods of determining unknown diffusion coefficients from similar foams of known data. The ageing program follows the trend of ageing very well. The prediction improves with time. This suggests that either the magnitude or relative importance of solid and radiative heat transfer is diminishing over time.

6) An optimization study over a presumed 15 year service-life for unfaced foams show that design must be aimed at diminishing the gas exchange. The optimal design density for a foam insulation over a 15 year service life is approximately 3 lb/ft^3. This can be compared to a 2 lb/ft^3 optimal density shown for the fresh, unaged foam.

References

[1] Page, M.C.,"Effects of Alternating Blowing Agents on the Aging of Closed-Cell Foam Insulation", M.S. Thesis, Dept. of Mechanical Engineering, MIT, 1991.

[2] Schuetz, M.A.,"Heat Transfer in Foam Insulation", M.S. Thesis, Dept. of Mechanical Engineering, MIT, 1982.

[3] Gibson, L.J. and Ashby, M.F.,Cellular Solids, Pergamon Press, New York, 1988.

[4] Ostrogorsgky, A.G.,"Aging of Polyurethane Foams", Ph.D. Thesis, Dept. of Mechanical Engineering, MIT, 1985

[5] Reitz, W.A.,"A Basic Study of Gas Diffusion in Foam Insulation", M.S. Thesis, Dept. of Mechanical Engineering, MIT, 1983.

[6] Sinofsky, M.,"Property Measurement and Thermal Performance of Foam Insulation", M.S. Thesis, Dept. of Mechanical Engineering, MIT, 1984.

[7] Foam tutorial session by Page.

[8] Personal communication; 8/91

[9 Siegel, R. and Howell, J.R.,Thermal Radiation Heat Transfer, Hemisphere Publishing Corp., New York, 1981.

[10] Class notes from 2.58, Spring 1991.

[11] Torpey, M.,"A Study of Radiation Heat Transfer Through Foam Insulation", M.S. Thesis, Dept. of Mechanical Engineering, MIT, 1987.

[12] Mozgowiec, M.,"The Use of Small Cells to Reduce Radiation Heat Transfer in Foam Insulation", M.S. Thesis, Dept. of Mechanical Engineering, MIT, 1990.

[13] Brehm, Timothy R. "Transient Measurement of Gas Permeability in Closed-Cell Insulation", M.S. Thesis, Dept. of Mechanical Engineering, MIT, 1989.

[14]Geankopolis,C.J.,Transport Processes, Allyn and Bacon Inc.,Newton, MA, 1983

[15] Underwood, E.E, Qualitative Stereology, Addison-Wesley Publishing Co., Reading , MA 1970

[16] Agnihotri, A.K. and Lemlich,R.,"Electrical Conductivity and the Distribution of Liquid in Polyhedral foam", Journal of Colloid and Interface Science, Vol. 84, No.1, 1981.

[17] McElroy, D.L., Graves, R.S., Weaver, F.J., "Thermal Resistance of Prototypical Cellular Plastic Roof Insulations", for 2nd Inter. Wkshp. on Long-Term Thermal Performance of Cell. Plastics, Niagra-On-The-Lake, June 5-7,1991

[18] Cunningham, A., and Sparrow, D. J., "Rigid Polyurethane Foam: What makes it the most effective insulant ?",*Cellular Plastics*, Vol. 5, 1986.

[19] Landon, S.J., and Lombardo, J.L.,"New Developments in Reduced CFC-11 Rigid Foam Appliance Systems", Proceedings of the SPI-33rd Annual Tecnical/Marketing Conference, Orlando, FL, Sept.30-Oct.3 1990, p.571.

[20] Blanpied, R.H., and Knis, S.A.,"The Technical Viability of Alternative Blowing Agents in Polyisocyanurate Roof Insulation Part 1: Processing and Physical Properties', Proceedings of the SPI-33rd Annual Tecnical/Marketing Conference, Orlando, FL, Sept.30-Oct.3 1990, p. 236

Appendix 1: Foam Data

Foam #	Description	Contact
1	UC†: Machine made: Surfactant L-5440	Kenrick Lewis
2	UC†: Machine made: Surfactant L-6900	"
3	UC†: Machine made: Surfactant L-6980	"
4	UC†: Lab made: Surfactant L-6900	"
5	UC†: Lab made: Surfactant L-6980	"
11	Mobay: NB 514756: Polyether-polyester -PMDI-CFC-11: ρf = 1.3 lbs/ft3	John Szabat
12	Mobay: NB 514756: Polyether-polyester -PMDI-CFC-11: ρf = 1.35 lbs/ft3	John Szabat
13	NB 1018117-2: Polyester-Mondur-MR200 -HCFC-123	"
21	ORNL¥: blown with CFC-11	Ron Graves
23	ORNL¥: blown with HCFC-123	"
25	ORNL¥: blown with HCFC-141B	"
27	ORNL¥: 50/50 HCFC-123 and 141B	"
28	ORNL¥: 65/35 HCFC-123 and 141B	"

† formulations may be found in reference 19

¥ formulations may be found in reference 20

Appendix 2: Ageing Correlation

Input Data for Ageing Program

In the form of:

thickness	# of nodes	
time in days	time interval	print time interval
Doc_{o2}	E/R_{co2}	initial PP of CO2 in closed-cell
Do_{o2}	E/R_{co2}	initial PP of O2 in closed-cell
Do_{n2}	E/R_{co2}	initial PP of N2 in closed-cell
Do_{ba}	E/R_{ba}	initial PP of BA in closed-cell
T1	T2	
k_{sol}	k_{rad}	

Foam 21

3.81	11	
600	5	1
0.0327	2482	1E-06
0.0109	2482	1E-06
0.0012	2482	1E-06
0.0153	2482	75000
298	298	
0.00203	0.00287	

(in metric units) W/m K

Foam 23

3.81	11	
600	5	1
0.0166	2210	1E-06
0.0055	2210	1E-06
0.0006	2210	1E-06
0.0081	3926	75000
298	298	
0.0219	0.0234	

Foam 25

3.81	11	
600	5	1
0.1567	3064	1E-06
0.0522	3064	1E-06
0.0058	3064	1E-06
0.0779	4783	75000
298	298	
0.00216	0.0026	

Foam 27

3.81	11	
600	5	1
0.0065	1972	1E-06
0.0022	1972	1E-06
0.0002	1972	1E-06
0.0033	3693	75000
298	298	
0.00218	0.0025	

Foam 28

3.81	11	
600	5	1
0.0294	1972	1E-06
0.0098	1972	1E-06
0.0011	1972	1E-06
0.0147	3693	75000
298	298	
0.00197	0.00274	

Appendix 3: Optimization Program

The optimization program

successive membrane model: Deff = 2*<l>/t *Dcw

Basically a geometry argument; the cell wall diffusion is assumed to remain constant. Thus, if either the diameter or the cell wall thickness are changed, then the effective diffusion is scaled up or down accordingly. The effective diffusion is related to the scaling coefficient Do by an Arhenius temperature dependence: Deff = Do*exp(-E/rT).
The temperature is constant and so are the activation energies, for the same sample. Any scaling changes made to the diffusion coefficient will directly affect the Do value.

>>>> Shall see how the time averaged conductivity behaves as a function of basic physical parameters which include the foam density, the fraction solid in the struts, and the mean cell diameter.

solid polymer conduction=	1.87 BTU IN/H FT2 F
stephan boltzmann	2E-09 BTU/FT2 F4
cell wall extinction coeff	4148 IN^-1
mean temperature	535 F
CFC-11, vapor density	0.4 lb/ft3
solid polymer density	77.5 lb/ft3

CFC-II blown foam: diffusion coefficient measured by Melissa Page at three Temp's:
.....can calculate the following values using the Arhenius expression for diffusion

for	CO2	Do=	0.0327 cm3/cm s	E/R=	2.48E+03
	CFC11	Do=	0.0153 cm3/cm s	E/R=	4.18E+03

constant fractions between CO2 and the other air components is assumed in this a
....those fractions are 1/3 and 1/27 for O2 and N2, respectively

..... and the foam had the following geometrical relationship:

<l>/t= 535 where <l> is the mean chord length and t is the cell wall thickness.

Nomenclature:
d=mean cell diameter, fs=fraction solid in the struts, pf= density of the foam, ∂=void fraction, ks=effective solid conductivity, kr=radiative conductivity, kg=15 year-time averaged gas conductivity, kT= time averaged effective foam conductivity, kI=initial

Relations:
ks=(1-∂)(2/3-fs/3)ksp where ksp is the solid polymer conductivity
kr=16/3*SB*Tm^3/(4/d*(fs pf/ps)^.5+pf/ps (1-fs)Kw)
kg,i is the CFC11 conductivity: .057 btu...
kI = ks + kr + kg,i
kT = ks + kr + kg

k's in BTU IN/FT2 H F4

d
0.1 mm

Trial 1

pf	fs	∂	<l>/t	Do's	E/R	ks	kr	kl
2	0.8	0.9792	481.88	0.029489	2482	1.55E-02	8.29E-03	8.08E-02
				0.00983	2482	kT	kg	
				0.001092	2482	2.06E-01	1.82E-01	
				0.013796	4176			

Trial 2

pf	fs	∂	<l>/t	Do's		ks	kr	kl
2.5	0.8	0.9728	367.14	0.022468	2482	2.04E-02	7.31E-03	8.47E-02
				0.007489	2482	kT	kg	
				0.000832	2482	2.09E-01	1.81E-01	
				0.010511	4176			

Trial 3

pf	fs	∂	<l>/t	Do's		ks	kr	kl
3	0.8	0.9663	296.54	0.018147	2482	2.52E-02	6.58E-03	8.88E-02
				0.006049	2482	kT	kg	
				0.000672	2482	2.14E-01	1.82E-01	
				0.00849	4176			

trial 4

pf	fs	∂	<l>/t	Do's		ks	kr	kl
4	0.8	0.9533	214.17	0.013106	2482	3.49E-02	5.57E-03	9.75E-02
				0.004369	2482	kT	kg	
				0.000485	2482	2.25E-01	1.84E-01	
				0.006132	4176			

Trial 5

pf	fs	∂	<l>/t	Do's		ks	kr	kl
1.75	0.8	0.9825	571.11	0.03495	2482	1.31E-02	8.94E-03	7.90E-02
				0.01165	2482	kT	kg	
				0.001294	2482	2.06E-01	1.84E-01	
				0.016351	4176			

trial 6

						ks	kr	kl
1.5	0.8	0.9857	700.91	0.042893	2482	1.07E-02	9.74E-03	7.74E-02
				0.014298	2482	kT	kg	
				0.001589	2482	2.06E-01	1.86E-01	
				0.020067	4176			

trial 7

						ks	kr	kl
1.25	0.8	0.989	907.06	0.055509	2482	8.25E-03	1.08E-02	7.60E-02
				0.018503	2482	kT	kg	
				0.002056	2482	2.07E-01	1.88E-01	
				0.025969	4176			

trial 8

						ks	kr	kl
1	0.8	0.9922	1285	0.078637	2482	5.82E-03	1.22E-02	7.50E-02
				0.026212	2482	kT	kg	
				0.002912	2482	2.08E-01	1.90E-01	
				0.036789	4176			

d
0.1 mm

Trial 1

pf	fs	∂	<l>/t	Do's	E/R	ks	kr	kl
2	0.5	0.9792	192.75	0.011796	2482	1.94E-02	8.22E-03	8.46E-02
				0.003932	2482	kT	kg	
				0.000437	2482	1.88E-01	1.60E-01	
				0.005518	4176			

Trial 2

pf	fs	∂	<l>/t	Do's		ks	kr	kl
2.5	0.5	0.9728	146.86	0.008987	2482	2.55E-02	7.09E-03	8.96E-02

				0.002996	2482	kT		kg	
				0.000333	2482	1.89E-01		1.56E-01	
				0.004205	4176				
Trial 3									
pf	fs	∂	<l>/t	Do's		ks		kr	kl
3	0.5	0.9663	118.62	0.007259	2482	3.15E-02		6.26E-03	9.48E-02
				0.00242	2482	kT		kg	
				0.000269	2482	4.15E-01		1.53E-01	
				0.003396	4176				
trial 4									
pf	fs	∂	<l>/t	Do's		ks		kr	kl
4	0.5	0.9533	85.667	0.005242	2482	4.37E-02		5.14E-03	1.06E-01
				0.001747	2482	kT		kg	
				0.000194	2482	1.98E-01		1.50E-01	
				0.002453	4176				
Trial 5									
pf	fs	∂	<l>/t	Do's		ks		kr	kl
1.75	0.5	0.9825	228.44	0.01398	2482	1.64E-02		8.97E-03	8.23E-02
				0.00466	2482	kT		kg	
				0.000518	2482	1.88E-01		1.63E-01	
				0.00654	4176				
trial 6						ks		kr	kl
1.5	0.5	0.9857	280.36	0.017157	2482	1.33E-02		9.91E-03	8.03E-02
				0.005719	2482	kT		kg	
				0.000635	2482	1.90E-01		1.67E-01	
				0.008027	4176				
trial 7						ks		kr	kl
1.25	0.5	0.989	362.82	0.022203	2482	1.03E-02		1.11E-02	7.84E-02
				0.007401	2482	kT		kg	
				0.000822	2482	1.94E-01		1.72E-01	
				0.010388	4176				
trial 8						ks		kr	kl
1	0.5	0.9922	514	0.031455	2482	7.28E-03		1.28E-02	7.71E-02
				0.010485	2482	kT		kg	
				0.001165	2482	1.98E-01		1.78E-01	
				0.014716	4176				

d									
0.2 mm									
Trial 1									
pf	fs	∂	<l>/t	Do's	E/R	ks		kr	kl
2	0.8	0.9792	481.88	0.029489	2482	1.55E-02		1.47E-02	8.72E-02
				0.00983	2482	kT		kg	
				0.001092	2482	2.20E-01		1.90E-01	
				0.013796	4176				
Trial 2									
pf	fs	∂	<l>/t	Do's		ks		kr	kl
2.5	0.8	0.9728	367.14	0.022468	2482	2.04E-02		1.28E-02	9.02E-02
				0.007489	2482	kT		kg	
				0.000832	2482	2.21E-01		1.88E-01	
				0.010511	4176				
Trial 3									
pf	fs	∂	<l>/t	Do's		ks		kr	kl
3	0.8	0.9663	296.54	0.018147	2482	2.52E-02		1.14E-02	9.37E-02
				0.006049	2482	kT		kg	
				0.000672	2482	2.24E-01		1.87E-01	
				0.00849	4176				
trial 4									
pf	fs	∂	<l>/t	Do's		ks		kr	kl
4	0.8	0.9533	214.17	0.013106	2482	3.49E-02		9.51E-03	1.01E-01

					0.004369	2482	kT	kg	
					0.000485	2482	2.33E-01	1.88E-01	
					0.006132	4176			
Trial 5									
pf	fs	∂	<I>/t	Do's		ks	kr	kl	
1.75	0.8	0.9825	571.11	0.03495	2482	1.31E-02	1.60E-02	8.61E-02	
				0.01165	2482	kT	kg		
				0.001294	2482	2.21E-01	1.91E-01		
				0.016351	4176				
trial 6						ks	kr	kl	
1.5	0.8	0.9857	700.91	0.042893	2482	1.07E-02	1.75E-02	8.52E-02	
				0.014298	2482	kT	kg		
				0.001589	2482	2.22E-01	1.94E-01		
				0.020067	4176				
trial 7						ks	kr	kl	
1.25	0.8	0.989	907.06	0.055509	2482	8.25E-03	1.95E-02	8.48E-02	
				0.018503	2482	kT	kg		
				0.002056	2482	2.25E-01	1.97E-01		
				0.025969	4176				
trial 8						ks	kr	kl	
1	0.8	0.9922	1285	0.078637	2482	5.82E-03	2.23E-02	8.51E-02	
				0.026212	2482	kT	kg		
				0.002912	2482	2.29E-01	2.01E-01		
				0.036789	4176				

d									
0.2 mm									
Trial 1									
pf	fs	∂	<I>/t	Do's	E/R	ks	kr	kl	
2	0.5	0.9792	192.75	0.011796	2482	1.94E-02	1.25E-02	8.89E-02	
				0.003932	2482	kT	kg		
				0.000437	2482	2.06E-01	1.74E-01		
				0.005518	4176				
Trial 2									
pf	fs	∂	<I>/t	Do's		ks	kr	kl	
2.5	0.5	0.9728	146.86	0.008987	2482	2.55E-02	1.06E-02	9.30E-02	
				0.002996	2482	kT	kg		
				0.000333	2482	2.10E-01	1.74E-01		
				0.004205	4176				
Trial 3									
pf	fs	∂	<I>/t	Do's		ks	kr	kl	
3	0.5	0.9663	118.62	0.007259	2482	3.15E-02	9.20E-03	9.77E-02	
				0.00242	2482	kT	kg		
				0.000269	2482	2.16E-01	1.76E-01		
				0.003396	4176				
trial 4									
pf	fs	∂	<I>/t	Do's		ks	kr	kl	
4	0.5	0.9533	85.667	0.005242	2482	4.37E-02	7.36E-03	1.08E-01	
				0.001747	2482	kT	kg		
				0.000194	2482	2.34E-01	1.83E-01		
				0.002453	4176				
Trial 5									
pf	fs	∂	<I>/t	Do's		ks	kr	kl	
1.75	0.5	0.9825	228.44	0.01398	2482	1.64E-02	1.38E-02	8.71E-02	
				0.00466	2482	kT	kg		
				0.000518	2482	2.06E-01	1.75E-01		
				0.00654	4176				
trial 6						ks	kr	kl	
1.5	0.5	0.9857	280.36	0.017157	2482	1.33E-02	1.54E-02	8.57E-02	
				0.005719	2482	kT	kg		

				0.000635	2482	2.07E-01	1.78E-01		
				0.008027	4176				
trial 7						ks	kr	kl	
1.25	0.5	0.989	362.82	0.022203	2482	1.03E-02	1.76E-02	8.49E-02	
				0.007401	2482	kT	kg		
				0.000822	2482	2.10E-01	1.82E-01		
				0.010388	4176				
trial 8						ks	kr	kl	
1	0.5	0.9922	514	0.031455	2482	7.28E-03	2.05E-02	8.48E-02	
				0.010485	2482	kT	kg		
				0.001165	2482	2.16E-01	1.89E-01		
				0.014716	4176				

d

0.5 mm

Trial 1

pf	fs	∂	<l>/t	Do's	E/R	ks	kr	kl	
2	0.8	0.9792	481.88	0.029489	2482	1.55E-02	2.74E-02	1.00E-01	
				0.00983	2482	kt	kg		
				0.001092	2482	2.46E-01	2.03E-01		
				0.013796	4176				

Trial 2

pf	fs	∂	<l>/t	Do's		ks	kr	kl	
2.5	0.8	0.9728	367.14	0.022468	2482	2.04E-02	2.34E-02	1.01E-01	
				0.007489	2482	kt	kg		
				0.000832	2482	2.43E-01	1.99E-01		
				0.010511	4176				

Trial 3

pf	fs	∂	<l>/t	Do's		ks	kr	kl	
3	0.8	0.9663	296.54	0.018147	2482	2.52E-02	2.05E-02	1.03E-01	
				0.006049	2482	kt	kg		
				0.000672	2482	2.42E-01	1.97E-01		
				0.00849	4176				

trial 4

pf	fs	∂	<l>/t	Do's		ks	kr	kl	
4	0.8	0.9533	214.17	0.013106	2482	3.49E-02	1.65E-02	1.08E-01	
				0.004369	2482	kt	kg		
				0.000485	2482	2.47E-01	1.96E-01		
				0.006132	4176				

Trial 5

pf	fs	∂	<l>/t	Do's		ks	kr	kl	
1.75	0.8	0.9825	571.11	0.03495	2482	1.31E-02	3.02E-02	1.00E-01	
				0.01165	2482	kt	kg		
				0.001294	2482	2.65E-01	2.22E-01		
				0.016351	4176				

trial 6

						ks	kr	kl	
1.5	0.8	0.9857	700.91	0.042893	2482	1.07E-02	3.36E-02	1.01E-01	
				0.014298	2482	kt	kg		
				0.001589	2482	2.55E-01	2.10E-01		
				0.020067	4176				

trial 7

						ks	kr	kl	
1.25	0.8	0.989	907.06	0.055509	2482	8.25E-03	3.81E-02	1.03E-01	
				0.018503	2482	kt	kg		
				0.002056	2482	2.63E-01	2.16E-01		
				0.025969	4176				

trial 8

						ks	kr	kl	
1	0.8	0.9922	1285	0.078637	2482	5.82E-03	4.43E-02	1.07E-01	
				0.026212	2482	kt	kg		
				0.002912	2482	2.74E-01	2.23E-01		
				0.036789	4176				

	d								
	0.3 mm								
Trial 1									
pf	fs	∂	<l>/t	Do's	E/R	ks	kr	kl	
2	0.5	0.9792	192.75	0.011796	2482	1.94E-02	1.51E-02	9.15E-02	
				0.003932	2482	kt	kg		
				0.000437	2482	2.18E-01	1.83E-01		
				0.005518	4176				
Trial 2									
pf	fs	∂	<l>/t	Do's		ks	kr	kl	
2.5	0.5	0.9728	146.86	0.008987	2482	2.55E-02	1.26E-02	9.51E-02	
				0.002996	2482	kt	kg		
				0.000333	2482	2.20E-01	1.81E-01		
				0.004205	4176				
Trial 3									
pf	fs	∂	<l>/t	Do's		ks	kr	kl	
3	0.5	0.9663	118.62	0.007259	2482	3.15E-02	1.09E-02	9.94E-02	
				0.00242	2482	kt	kg		
				0.000269	2482	2.24E-01	1.81E-01		
				0.003396	4176				
trial 4									
pf	fs	∂	<l>/t	Do's		ks	kr	kl	
4	0.5	0.9533	85.667	0.005242	2482	4.37E-02	8.60E-03	1.09E-01	
				0.001747	2482	kt	kg		
				0.000194	2482	2.39E-01	1.87E-01		
				0.002453	4176				
Trial 5									
pf	fs	∂	<l>/t	Do's		ks	kr	kl	
1.75	0.5	0.9825	228.44	0.01398	2482	1.64E-02	1.68E-02	9.01E-02	
				0.00466	2482	kt	kg		
				0.000518	2482	2.19E-01	1.86E-01		
				0.00654	4176				
trial 6						ks	kr	kl	
1.5	0.5	0.9857	280.36	0.017157	2482	1.33E-02	1.89E-02	8.92E-02	
				0.005719	2482	kt	kg		
				0.000635	2482	2.22E-01	1.90E-01		
				0.008027	4176				
trial 7						ks	kr	kl	
1.25	0.5	0.989	362.82	0.022203	2482	1.03E-02	2.17E-02	8.90E-02	
				0.007401	2482	kt	kg		
				0.000822	2482	2.29E-01	1.97E-01		
				0.010388	4176				
trial 8						ks	kr	kl	
1	0.5	0.9922	514	0.031455	2482	7.28E-03	2.57E-02	9.00E-02	
				0.010485	2482	kt	kg		
				0.001165	2482	2.40E-01	2.07E-01		
				0.014716	4176				

Appendix 4: Rosseland Mean Computer Code

```
c
      program rosseland
      real tr(15,2000),trs(15),kbeta,krb,w(15),kfeta,krf,a,b
c
c     Each file reresents spectral transmission for a single sample thickne
c
      open (10,file='micell10.asc',status='old')
      open (11,file='miccell4.asc',status='old')
      open (12,file='miccell7.asc',status='old')
      open (13,file='miccell8.asc',status='old')
      open (14,file='miccell9.asc',status='old')
c
      data c1,c2,t/.18892e8,25898,528./
      data sb,n,deta/1.712e-9,138,11.5744/
      pi=acos(-1.)
      nsam=5
      write(*,5)
 5    format (t4,'K(forced)',t18,'Corr.',t30,'K(best fit)',t45,'Corr.')
c
c     Slice thicknesses are stored in an array
c
      do 10 i1=10,nsam+9
         read(i1,*)w(i1-9)
 10   continue
c
c     transmissivities are stored in a two dimensional array
c
c
      do 30 iw=1,380
         do 20 is=10,(nsam+9)
            i1=is-9
            i2=iw-242
            if (iw.le.242) then
               read(is,*)q
            else
               read(is,*)tr(i1,i2)
            endif
 20      continue
 30   continue
c
c     la numerical integration
c
      do 50 j1=1,n
         do 40 j2=1,nsam
            trs(j2)=tr(j2,j1)
 40      continue
c
         call exc(trs,w,nsam,kfeta,corrf,kbeta,corrb)
```

```
c
          eta=2000.-j1*deta
          a=(pi*c1*c2*((eta/10000)**4))/(2.*sb*(t**5))
          b=exp(c2*(eta/10000)/t)
          sumkb=sumkb+((a*b)/(kbeta*(b-1.)*(b-1.)))*deta
          sumkf=sumkf+((a*b)/(kfeta*(b-1.)*(b-1.)))*deta
          sum=sum+((a*b)/((b-1.)*(b-1.)))*deta
c
c
c
          sumcorrf=sumcorrf+corrf
          sumcorrb=sumcorrb+corrb




c
          write(6,45) kfeta,corrf,kbeta,corrb
 45       format(t6,f6.2,t17,f6.4,t33,f6.2,t44,f6.4)
 50     continue
c
c      best and force fit total extinction values
c
          krf=sum/sumkf
          krb=sum/sumkb
c
          write (6,60)krf
          write (6,70)sumcorrf/n
          write (6,80)krb
          write(6,70)sumcorrb/n
 60       format(//,t3,'extinction coefficient - force fit: ',f6.2)
 70       format(t3,'average correlation: ',f6.4//)
 80       format(t3,'extinction coefficient - actual fit: ',f6.2)
          stop
          end
c
c
c      subroutine exc
c
c
          subroutine exc(tau,x,n,kf,rf,kb,rb)
          real kb,tau(15),x(15),kf,icept
          sumx2=0
          sumxy=0
          sumx=0
          sumy=0
          sumym=0
          sumycb=0
          sumycf=0
c
```

```
c
      do 100 j=1,n
         if(tau(j) .le. .0001) then
            tau(j)=.0001
         endif
         y= -log(tau(j))
         sumx2=sumx2+(x(j)*x(j))
         sumxy=sumxy+(y*x(j))
         sumy=sumy+y
         sumx=sumx+x(j)
 100  continue
c
      kf=sumxy/sumx2
      kb=(n*sumxy-sumx*sumy)/(n*sumx2-sumx*sumx)
c
c
      icept=(sumy*sumx2-sumxy*sumx)/(n*sumx2-sumx*sumx)
      ym=sumy/n
c
c     Least squares data analysis for correlation coefficients
c
      do 110 i=1,n
         if(tau(i) .le. .0001) then
            tau(i)=.0001
         endif
         y=-log(tau(i))
         ycf=kf*x(i)
         ycb=kb*x(i)+icept
         sumym=sumym+(y-ym)*(y-ym)
         sumycb=sumycb+(y-ycb)*(y-ycb)
         sumycf=sumycf+(y-ycf)*(y-ycf)
 110  continue


      sigy2=sumym/(n-1)
      sigyxb2=sumycb/(n-2)
      sigyxf2=sumycf/(n-2)
      write (6,112)sigyxb2,sigyxf2,sigy2
 112  format(t5,f5.4,t15,f5.4,t25,f5.4)
      if (sigyxf2 .ge. sigy2) then
         rf=0.
         goto 120
      endif
c
c     correlation coefficients
c
      rf=(1.-(sigyxf2/sigy2))**0.5
 120  rb=(1.-(sigyxb2/sigy2))**0.5
      return
      end
```

Appendix 5: Ageing Computer Code

```
C
C  WRITTEN BY: A. OSTROGORSKY, M.I.T., FEB. 1985
C MODIFIED BY: T. BREHM, M.I.T., AUG. 1987
C  Modified by : L. Glicksman M.I.T. December 20, 1989
C
C THIS IS THE AGE PROGRAM.
C AGE COMPUTES THE 1-D TIME CHANGE OF THE GAS
C COMPOSITION AND GAS CONDUCTIVITIY INSIDE OF
C AN INFINITE CLOSED CELL FOAM SLAB, AND ADDS
C IT TO  THE CONDUCTIVITY OF SOLID AND CONDUCTANCE
C DUE TO RADIATION TO PRODUCE A PLOT OF EFFECTIVE
C FOAM CONDUCTANCE AS A FUNCTION OF TIME.
C

      COMMON/BLK1/  PP(4,5,51),PTOT(51),TT(5,51)
      COMMON/BLK2/  DF(4,51),PEO(4),E(4)
      COMMON/BLK3/  GASK(51),WMOL(4),S(4),SS(4,4)
      COMMON/BLK4/  NZ,DZ,NT,DT
      COMMON/BLK5/  CO2,O2,N2,FR

      REAL  PATM(4),THICK,MAXTIME,DTI,PDIFF,PRATIO
      REAL  KSOL,KRAD,KGAVG,KGSUM,KFOAM,KNODE,TIME
      REAL  QFLUX,RV,RVT,TPRINT
      INTEGER  I,IZ

      WRITE(6,*)'INITIALIZING...'
      WRITE(6,*)'OUTPUT FILE NAME, E.G. AGE.OUT'


C SET UP INPUT AND OUTPUT FILES
      OPEN(UNIT=10,FILE='AGE.DAT',STATUS='OLD')
      OPEN(UNIT=11,FILE=' ',STATUS='NEW')

      WRITE(6,*)'ENTER 1 TO SUPRESS PARTIAL PRES. OUTPUT'
      READ(5,*) PFLAG

C SYMBOLIC ARRAY INDICES
      CO2=1
      O2=2
      N2=3
      FR=4
```

```
C MOLECULAR WEIGHTS:
      WMOL(CO2)=44.0
      WMOL(O2)=32.0
      WMOL(N2)=28.0
      WMOL(FR)=137.4

C CONSTANTS FOR KG MIXTURE
      S(CO2)=1.5*(273.-78.476)
      S(O2)=1.5*(273.-182.962)
      S(N2)=1.5*(273.-195.8)
      S(FR)=1.5*(273.+10.)
      DO 20 I=1,4
         DO 10 J=1,4
            SS(I,J)=SQRT(S(I)*S(J))
10       CONTINUE
20    CONTINUE

C READ THE INPUT FILE
      WRITE(6,*)'READING DATA FROM FILE "AGE.DAT"...'
      READ(10,*)THICK,NZ,




     1          MAXTIME,DTI,TPRINT,

     1          PEO(CO2),E(CO2),PP(CO2,1,2),
     1          PEO(O2),E(O2),PP(O2,1,2),
     1          PEO(N2),E(N2),PP(N2,1,2),
     1          PEO(FR),E(FR),PP(FR,1,2),
     1          TT(1,1),TT(1,NZ),
     1          KSOL,KRAD
C              Thickness (cm), Number of nodes= number of div's +1
C              MAXIMUM TIME DAYS, TIME INTERVAL (DAYS), PRINT TIME INTERVAL
C              PP: partial pressure (pascals),
C              PP(component,time index,space index)
C              TT: temp (K)  TT(time index,space index)
c              KSOL,KRAD: solid and radiation k (W/M C)

C CONVERT INPUT DATA TO USEABLE FORM
      IF(NZ.GT.51)NZ=51
      DZ=THICK/(NZ-1)
      NT=MAXTIME/DTI
      DTI=3600.*24.*DTI
      MAXTIME=3600.*24.*MAXTIME
      TPRINT=TPRINT*3600.*24.

C SET INTIAL FOAM TO STANDARD TEMP
      DO 51 IZ=2,NZ-1
         TT(1,IZ)=298
51    CONTINUE
```

```
C CALCULATE IMPOSED TEMPERATURE PROFILE
      TT(2,1)=TT(1,1)
      DO 50 IZ=2,NZ-1
         TT(2,IZ)=TT(1,1)+(IZ-1)*(TT(1,NZ)-TT(1,1))/(NZ-1)
50    CONTINUE
      TT(2,NZ)=TT(1,NZ)

C SET PARTIAL PRESSURES OUTSIDE THE FOAM
      PPP=1.0132E+5
      PATM(CO2)=.000314
      PATM(O2)=.2095
      PATM(N2)=.78084
      PATM(FR)=0.0
      DO 25 I=1,4
         PP(I,1,1)=PATM(I)*PPP
         PP(I,1,NZ)=PATM(I)*PPP
25    CONTINUE

C SET INITIAL PARTIAL PRESSURES INSIDE THE FOAM
      DO 40 IZ=3,NZ-1
         DO 30 I=1,4
            PP(I,1,IZ)=PP(I,1,2)
30       CONTINUE
40    CONTINUE

C WRITE INITIAL HEADER TO OUTPUT FILE
      WRITE(11,*)' Thickness(cm),Number of nodes,d(thick) (cm)  '
      WRITE(11,*)THICK,NZ,DZ
      WRITE(11,*)'maximum time (days) , d(time) (days) '
      WRITE(11,*)MAXTIME/3600/24,DTI/3600/24
      Write(11,*)'Pe0    E       Initial Partial Pressure(pascals) '
      DO 41 I=1,4
         WRITE(11,*)PEO(I),E(I),PP(I,1,2)
41    CONTINUE
      DO 42 IZ=1,NZ


         WRITE(11,*)TT(2,IZ)
42    CONTINUE
      WRITE(11,*)'SOLID CONDUCTION       RADIATION  (W/M C)'
      WRITE(11,*)KSOL,KRAD

C SET LOOP VARIABLES TO BEGIN TIME ITERATIONS
      DT=DTI
      IT=0
      TIME=0
      WRITE(6,*)'STARTING TIME ITERATIONS...'
      WRITE(6,*)

C UPDATE LOOP VARIABLES FOR THIS TIME THROUGH
1000  CONTINUE
      IT=IT+1
      IF(IT .LT. 4) GOTO 1006
       IT = IT - 1
```

```
       DO 1005 NIT=IT-1,IT
        DO 1005 NONZ=1,NZ
         DO 1005 I=1,4
          PP(I,NIT,NONZ) = PP(I,NIT+1,NONZ)
1005    CONTINUE
1006    TIME=TIME+DT
C       TIME IN SECONDS
      IF(TIME.GT.MAXTIME) GOTO 2000


C SET THE B.C.'S
C   PRESSURE:
      DO 55 I=1,4
         PP(I,IT+1,1)=PP(I,1,1)
         PP(I,IT+1,NZ)=PP(I,1,1)
55    CONTINUE
C   TEMPERATURE:
      TT(IT+1,1)=TT(1,1)
      TT(IT+1,NZ)=TT(1,NZ)

C COMPUTE PRESSURE CHANGE DUE TO TEMPERATURE CHANGE
      DO 70 IZ=2,NZ-1
         DO 60 I=1,4
            PP(I,IT,IZ)=PP(I,IT,IZ)*TT(IT+1,IZ)/TT(IT,IZ)
60       CONTINUE
70    CONTINUE

C COMPUTE THE PRESSURE CHANGE DUE TO DIFFUSION
      CALL PPRESS(IT)

C COMPUTE THE CONDUCTIVITY OF THE GAS MIXTURE
      CALL KMIX(IT)
      KGSUM=0.0
      DO 80 IZ=2,NZ-1
         KGSUM=KGSUM+GASK(IZ)
80    CONTINUE
      KGAVG=KGSUM/(NZ-2)
      KFOAM=KSOL+KRAD+KGAVG

C COMPUTE THE FOAM RESISTANCE, HEAT FLUX, AND NEW TEMP PROFILE
      RV=0.0
      DO 90 IZ=2,NZ-1
         RV=RV+DZ/GASK(IZ)
90    CONTINUE
      RVT=1/(1/RV+(KSOL+KRAD)/THICK)
      QFLUX=(TT(IT+1,NZ)-TT(IT+1,1))/RVT
```

```
      DO 100 IZ=2,NZ-1
         KNODE=(GASK(IZ-1)+GASK(IZ))/2.+(KSOL+KRAD)/NZ
         TT(IT+2,IZ)=TT(IT+1,IZ-1)+QFLUX*DZ/KNODE
100   CONTINUE

C      PTIME = PTIME + DT
C      IF(PTIME .LT. TPRINT .AND. TIME .GT. DT) GOTO 111
C      PTIME = 0
      IF ( TIME - DT .EQ. 0 )  GOTO 3333
      IF ( AINT(TIME/TPRINT) .EQ. AINT ((TIME-DT)/TPRINT)) GOTO 111
C      IF (TIME .LE. DT) PTIME=DTI
3333  WRITE(6,1001)'TIME (DAYS) = ',TIME/3600/24,' K(BTU-IN/HRFT2F)= ',
     1  KFOAM/1.7307*12
1001  FORMAT('+',A,F8.1,A,F12.5)
      WRITE (6,*) ' '

C WRITE LOOP RESULTS TO OUTPUT FILE
      IF ( PFLAG .NE. 1 .OR. ILOOP .EQ. 0 ) THEN
      ILOOP = 1
      WRITE(11,*)'  '
      WRITE(11,*)'Time(days) Gas k(W/M C) Foam k(W/M C) Foam k(BTU-in/hr
     1 ft2 F) TIME/THCK2'
C       TIME/THCK2   (DAYS/CM2)
      ENDIF
      WRITE(11,3001)TIME/3600/24,KGAVG,KFOAM,KFOAM/1.7307*12,TIME/3600
     1 /24/THICK**2
3001  FORMAT(5G13.4)
      IF (PFLAG .EQ. 1) GOTO 111
      WRITE(11,*)'T (C) p(CO2) (pascals) p(O2)    p(N2)     p(R-11)  Gas
     1 k (W/M C)'
      DO 110 IZ=1,NZ
         WRITE(11,3002)TT(IT+1,IZ)-273,PP(CO2,IT,IZ),PP(O2,IT,IZ),
     1              PP(N2,IT,IZ),PP(FR,IT,IZ),GASK(IZ)
3002  FORMAT(1X,6G10.3)
110   CONTINUE
111   CONTINUE

C EVALUATE LOOP VARIABLES FOR EXIT CONDITION
      IF(DT.GT.8.6E+6)GOTO 200
      PDIFF=ABS(PP(N2,IT+1,NZ/2)-PP(N2,IT,NZ/2))
      IF(PDIFF.NE.0)PRATIO=PP(N2,IT,NZ/2)/PDIFF
      IF(PDIFF.EQ.0)PRATIO=9
      IF(PRATIO .LT. 4) THEN
        PRATIO = 0
      ELSE
        PRATIO = 4
      END IF
      DT=(1+PRATIO)*DTI
200   IF(DT.GT.8.64E+6)DT=8.64E+6
      IF(IT.GE.200)THEN
         WRITE(6,2001)' MEMORY FULL: STOPPED AT ',TIME/3600/24,' DAYS'
```

```
2001      FORMAT(A,F8.1,A)
          GOTO 2000
       ENDIF
       GO TO 1000
2000   CONTINUE

C MARK END OF OUTPUT FILE
       WRITE(11,*)0,0,0,0,0,0
       WRITE(11,*)
       WRITE(6,*)'ALL DONE.'

C END OF MAIN PROGRAM



       STOP
       END


CCCCCCCCCCCCCCCCCCCCCCCCCCCCCCCCCCCCCCCCCCCCCCCCCCCCCCCCCCCCCCCCCCCCCCCCCCCCCCCC
C
C
       SUBROUTINE PPRESS(IT)
C
C THIS SUBROUTINE COMPUTES THE CHANGE OF GAS PARTIAL PRESSURE
C WITH TIME
C
       REAL  AP(51),Q(51),X(51),A(51),B(51),C(51)
       REAL  L(51),D(51),U(51)

       COMMON/BLK1/  PP(4,5,51),PTOT(51),TT(5,51)
       COMMON/BLK2/  DF(4,51),PEO(4),E(4)
       COMMON/BLK4/  NZ,DZ,NT,DT
       COMMON/BLK5/  CO2,O2,N2,FR

C SET CONSTANT MATRIX COEFFICIENTS
       DO 15 IZ=1,NZ
          B(IZ)=1
          C(IZ)=1
15     CONTINUE

C COMPUTE DIFFUSION COEFFICIENTS AS FUNCTION OF TEMPERATURE
       DO 20 IZ=2,NZ-1
          DO 10 I=1,4
             DF(I,IZ)=PEO(I)*EXP(-E(I)/TT(IT+1,IZ))*TT(IT+1,IZ)/298.
10        CONTINUE
20     CONTINUE

C COMPUTE THE PRESSURE CHANGES
       DO 50 I=1,4
          AP(2)=DZ*DZ/(DT*DF(I,2)*.5)
          A(2)=-(2.+AP(2))
          AP(NZ-1)=DZ*DZ/(DT*DF(I,NZ-1)*.5)
          A(NZ-1)=-(2.+AP(NZ-1))
```

```
      Q(2)=-2.*PP(I,IT,1)+PP(I,IT,2)*(2.-AP(2))-PP(I,IT,3)
      Q(NZ-1)=-PP(I,IT,NZ-2)+PP(I,IT,NZ-1)*(2.-AP(NZ-1))
     1        -2.*PP(I,IT,NZ)
      DO 30 IZ=3,NZ-2
         AP(IZ)=DZ*DZ/(DT*DF(I,IZ)*.5)
         A(IZ)=-(2.+AP(IZ))
         Q(IZ)=-PP(I,IT,IZ-1)+PP(I,IT,IZ)*(2.-AP(IZ))
     1          -PP(I,IT,IZ+1)
30    CONTINUE
      CALL LUDE(A,B,C,L,D,U,NZ)
      CALL  FBACK(L,D,U,Q,X,NZ)
      DO 40 IZ=2,NZ-1
         PP(I,IT+1,IZ)=X(IZ)
40    CONTINUE
50  CONTINUE

C COMPUTE THE TOTAL PRESSURE
    DO 70 IZ=1,NZ
      PTOT(IZ)=0.0
      DO 60 I=1,4
         PTOT(IZ)=PTOT(IZ)+PP(I,IT+1,IZ)
60    CONTINUE
70  CONTINUE


    RETURN
    END

CCCCCCCCCCCCCCCCCCCCCCCCCCCCCCCCCCCCCCCCCCCCCCCCCCCCCCCCCCCCCCCCCCCCCCCCCCCC
C
      SUBROUTINE KMIX(IT)
C
C THE SUBROUTINE COMPUTES THE CONDUCTIVITY OF THE GAS MIXTURE
C INSIDE THE CLOSED FOAM CELLS AS A FUNCTION OF GAS COMPOSITION
C AT EACH NODE.
C
      REAL ETA(4),YA(4),X(4,51),K(4),AA(4,4)
      INTEGER  IT,IZ,I,J

      COMMON/BLK1/  PP(4,5,51),PTOT(51),TT(5,51)
      COMMON/BLK3/  GASK(51),WMOL(4),S(4),SS(4,4)
      COMMON/BLK4/  NZ,DZ,NT,DT
      COMMON/BLK5/  CO2,O2,N2,FR

C COMPUTE MOL FRACTIONS:
      DO 15 IZ=1,NZ
         DO 10 I=1,4
            X(I,IZ)=PP(I,IT+1,IZ)/PTOT(IZ)
10       CONTINUE
15    CONTINUE
```

```
C MIXTURE CONDUCTIVITY GASK(IZ):
      DO 40 IZ=1,NZ
         ETA(CO2)=(14.958+(TT(IT,IZ)-300.)/50.*2.247)*1.E-6
         ETA(O2)=(20.63+(TT(IT,IZ)-300.)/50.*2.53)*1.E-6
         ETA(N2)=(17.84+(TT(IT,IZ)-300.)/100.*4.14)*1.E-6
         ETA(FR)=20.000E-6
         DO 30 I=1,4
            DO 20 J=1,4
               IF(I.EQ.J)AA(I,J)=0.0
               IF(I.EQ.J)GOTO 20
               AA(I,J)=.25*(1.+SQRT(ETA(I)/ETA(J)*
     1                 (WMOL(J)/WMOL(I))**.75*
     1                 (TT(IT,IZ)+S(I))/(TT(IT,IZ)+S(J))))**2.*
     1                 (TT(IT,IZ)+SS(I,J))/(TT(IT,IZ)+S(I))
20          CONTINUE
         YA(I)=X(CO2,IZ)*AA(I,CO2)+X(O2,IZ)*AA(I,O2)
     1         +X(N2,IZ)*AA(I,N2)+X(FR,IZ)*AA(I,FR)
30    CONTINUE
      K(CO2)=.016572+(TT(IT,IZ)-300.)/50.*.003898
      K(O2)=.02676+(TT(IT,IZ)-300.)/50.*.00394
      K(N2)=.02620+(TT(IT,IZ)-300.)/100.*.00715
      K(FR)=8.3022E-3+(9.426E-3-8.3022E-3)/27.8*(TT(IT,IZ)-310.93)
      GASK(IZ)=K(CO2)*X(CO2,IZ)/(X(CO2,IZ)+YA(1))
     1       +K(O2)*X(O2,IZ)/(X(O2,IZ)+YA(2))
     1       +K(N2)*X(N2,IZ)/(X(N2,IZ)+YA(3))
     1       +K(FR)*X(FR,IZ)/(X(FR,IZ)+YA(4))
40    CONTINUE

C      WRITE(6,*)GASK(1)

      RETURN
      END


CCCCCCCCCCCCCCCCCCCCCCCCCCCCCCCCCCCCCCCCCCCCCCCCCCCCCCCCCCCCCCCCCCCCCCC
C
```

```
      SUBROUTINE LUDE(A,B,C,L,D,U,N)
C
C THIS ROUTINE DECOMPODES A TRIDIAGONAL MATRIX [ABC] INTO LOWER AND UPPER
C DIAGONAL MATRICES [L] AND [DU].
C
      REAL A(N),B(N),C(N),L(N),D(N),U(N)
      INTEGER  I

      D(2)=A(2)
      U(2)=C(2)
      DO 10 I=3,N-1
         L(I)=B(I)/D(I-1)
         D(I)=A(I)-L(I)*U(I-1)
         U(I)=C(I)
10    CONTINUE

      RETURN
      END

CCCCCCCCCCCCCCCCCCCCCCCCCCCCCCCCCCCCCCCCCCCCCCCCCCCCCCCCCCCCCCCCCCCCCCCCCCCCCCC
C
      SUBROUTINE FBACK(L,D,U,Q,X,N)
C
C THIS ROUTINE PERFORMS FORWARD/BACKWARD SOLVE OF MATRIX SYSTEM
C [L][U][X]=[Q].
C
      REAL L(N),D(N),U(N),Q(N),X(N)
      INTEGER  I

      X(2)=Q(2)
      DO 10 I=3,N-1
         X(I)=Q(I)-L(I)*X(I-1)
10    CONTINUE
      X(N-1)=X(N-1)/D(N-1)
      DO 20 I=N-2,2,-1
         X(I)=(X(I)-U(I)*X(I+1))/D(I)
20    CONTINUE

      RETURN
      END
```